



# A biophysical approach using water deficit factor for daily estimations of evapotranspiration and CO<sub>2</sub> uptake in Mediterranean environments

David Helman<sup>1</sup>, Itamar M. Lensky<sup>1</sup>, Yagil Osem<sup>2</sup>, Shani Rohatyn<sup>3</sup>, Eyal Rotenberg<sup>3</sup>, and Dan Yakir<sup>3</sup>

<sup>1</sup>Department of Geography and Environment, Bar-Ilan University, Ramat Gan 52900, Israel

<sup>2</sup>Department of Natural Resources, Agricultural Research Organization, Volcani Center, Bet Dagan 50250, Israel

<sup>3</sup>Earth and Planetary Sciences, Weizmann Institute of Science, Rehovot 76100, Israel

Correspondence to: David Helman (davidhelman.biu@gmail.com, david.helman@biu.ac.il)

Received: 22 May 2017 – Discussion started: 23 May 2017

Revised: 26 July 2017 – Accepted: 10 August 2017 – Published: 7 September 2017

**Abstract.** Estimations of ecosystem-level evapotranspiration (ET) and CO<sub>2</sub> uptake in water-limited environments are scarce and scaling up ground-level measurements is not straightforward. A biophysical approach using remote sensing (RS) and meteorological data (RS–Met) is adjusted to extreme high-energy water-limited Mediterranean ecosystems that suffer from continuous stress conditions to provide daily estimations of ET and CO<sub>2</sub> uptake (measured as gross primary production, GPP) at a spatial resolution of 250 m. The RS–Met was adjusted using a seasonal water deficit factor ( $f_{WD}$ ) based on daily rainfall, temperature and radiation data. We validated our adjusted RS–Met with eddy covariance flux measurements using a newly developed mobile lab system and the single active FLUXNET station operating in this region (Yatir pine forest station) at a total of seven forest and non-forest sites across a climatic transect in Israel (280–770 mm yr<sup>−1</sup>). RS–Met was also compared to the satellite-borne MODIS-based ET and GPP products (MOD16 and MOD17, respectively) at these sites.

Results show that the inclusion of the  $f_{WD}$  significantly improved the model, with  $R = 0.64$ – $0.91$  for the ET-adjusted model (compared to  $0.05$ – $0.80$  for the unadjusted model) and  $R = 0.72$ – $0.92$  for the adjusted GPP model (compared to  $R = 0.56$ – $0.90$  of the non-adjusted model). The RS–Met (with the  $f_{WD}$ ) successfully tracked observed changes in ET and GPP between dry and wet seasons across the sites. ET and GPP estimates from the adjusted RS–Met also agreed well with eddy covariance estimates on an annual timescale at the FLUXNET station of Yatir ( $266 \pm 61$  vs.  $257 \pm 58$  mm yr<sup>−1</sup> and  $765 \pm 112$  vs.

$748 \pm 124$  gC m<sup>−2</sup> yr<sup>−1</sup> for ET and GPP, respectively). Comparison with MODIS products showed consistently lower estimates from the MODIS-based models, particularly at the forest sites. Using the adjusted RS–Met, we show that afforestation significantly increased the water use efficiency (the ratio of carbon uptake to ET) in this region, with the positive effect decreasing when moving from dry to more humid environments, strengthening the importance of drylands afforestation. This simple yet robust biophysical approach shows promise for reliable ecosystem-level estimations of ET and CO<sub>2</sub> uptake in extreme high-energy water-limited environments.

## 1 Introduction

Assessing the water use and carbon uptake in terrestrial ecosystems is important for monitoring biosphere responses to climate change (Ciais et al., 2005; Jung et al., 2010; Reichstein et al., 2013). Accurate estimations of evapotranspiration (ET) and gross primary production (GPP), as a measure of the CO<sub>2</sub> uptake, usually require the integration of extensive meteorological, flux and field-based data (e.g., Wang et al., 2014; Kool et al., 2014). However, scaling up field-based measurements to the ecosystem level is not straightforward and requires the use of complex models (Way et al., 2015).

Currently, the eddy covariance (EC) technique is the most direct method for measuring carbon and water vapor fluxes at the ecosystem level (Baldocchi, 2003). The EC approach benefits from continuous temporal coverage; cur-

rently (April, 2017), there are more than 560 active EC sites across the globe as part of the FLUXNET program (<http://fluxnet.ornl.gov>). However, there are also some practical and technical limitations. The EC measurement is representative of a relatively small area ( $< 2 \text{ km}^2$ ), and the application of the EC approach is limited to relatively homogeneous and flat terrains. Additionally, most EC towers are concentrated in the US, Europe and Asia, with poor coverage in water-limited regions, such as North Africa and the eastern Mediterranean (Schimel et al., 2015).

Remote-sensing-based models (RS models) have been used to overcome some of the limitations of EC, complementing the information derived from the flux towers. In contrast to process-driven models, RS models benefit from continuous, direct observation of the Earth's surface, acquiring data at a relatively high spatial resolution and with full regional to global coverage. Many RS models for the estimation of ET and GPP exist (see reviews in Kalma et al., 2008, and Hilker et al., 2008), but these algorithms are too complex and most of the models are not provided as accessible products for researchers outside the remote sensing community. Particular exceptions are the satellite-borne MODIS-based ET and GPP products (MOD16 and MOD17), which provide 8-day ET and GPP estimates at 1 km for 2000–2015, globally (Mu et al., 2007, 2011, Running et al., 2000, 2004).

In the past decade, several simple biophysical ET and GPP models based on vegetation indices (from satellite data) have emerged, offering assessment at relatively high to moderate spatial and temporal resolutions with an acceptable accuracy (i.e., daily estimates at 250 m; see, e.g., Veroustraete et al., 2002; Sims et al., 2008; Maselli et al., 2009, 2014; and review of ET models in Glenn et al., 2010). One of those models is the ET model based on the FAO-56 formulation (Allen et al., 1998). The FAO-56 formulation states that the actual ET of irrigated crops can be determined from the reference ET ( $ET_o$ ) corrected with crop coefficient  $K_c$  values (see Eq. 2). The  $K_c$  varies mainly with specific plant species characteristics, which enables the transfer of standard  $K_c$  values among locations and environments (Allen et al., 2006).

The remote-sensing version of this formulation uses a function of satellite-derived vegetation index, usually the normalized difference vegetation index (NDVI), as a substitute for the crop coefficient. Being a measure of the green plant biomass and the ecosystem leaf area, the NDVI is often used as a surrogate for plant transpiration and rainfall interception capacity (Glenn et al., 2010). Additionally, the NDVI is closely related to the radiation absorbed by the plant and to its photosynthetic capacity (Gamon et al., 1995). However, the direct detection, through NDVI, of the abovementioned parameters on a seasonal timescale is still challenging and usually requires additional meteorological information (Helman et al., 2015a). The RS model based on the FAO-56 formulation combines the two sources of information, satellite and meteorological, providing a daily estimation of actual ET. This model, originally proposed for croplands and other

managed vegetation systems (Allen et al., 1998; Glenn et al., 2010), was recently adjusted for applications in natural vegetation systems (Maselli et al., 2014).

For the estimation of GPP, a simple but robust biophysical GPP model is the one based on the radiation use efficiency (RUE) model proposed by Monteith (1977). The classical Monteith-type model depends on the absorbed radiation and on the efficiency of the vegetation at converting this radiation into carbon-based compounds. Accordingly, this Monteith-based model is driven by radiation and temperature data, acquired from meteorological stations, and by the fraction of absorbed photosynthetically active radiation ( $f_{APAR}$ ), which can be calculated from the satellite-derived NDVI. A major challenge in this model, however, is the estimation of the RUE, a key component of the model, which usually depends on plant species type and environmental conditions. Currently, the conventional procedure is to use a plant-species-dependent maximum RUE from a lookup table and adjust it for seasonal changes using some sort of a factor that changes throughout the season based on meteorological data (Running et al., 2004; Zhao and Running, 2010).

Though simple, both ET and GPP models (hereafter RS–Met) were shown to be promising in accurately assessing daily ET and GPP at a relatively high spatial resolution ( $< 1 \text{ km}$ ; Helman et al., 2017a; Maselli et al., 2014, 2006; Veroustraete et al., 2002). However, the use of the RS–Met is limited to ecosystems under normally non-stressful conditions because there is no accurate representation of water availability in these models. Recently, the incorporation of a water-deficit factor ( $f_{WD}$ ) in these models was proposed by Maselli et al. (2009, 2014), adjusting for short-term stress conditions in natural water-limited ecosystems. The proposed  $f_{WD}$  is based only on daily rainfall data and daily potential ET calculated from temperature and/or incoming radiation. The RS–Met with the addition of the  $f_{WD}$  was successfully validated against EC-derived estimates of ET and GPP at several sites in Italy (Maselli et al., 2014, 2009, 2006).

However, the RS–Met approach has never been tested in extreme high-energy water-limited environments such as those in the eastern Mediterranean. Currently, there is only one active FLUXNET station in the entire eastern Mediterranean (Yatir forest, southern Israel; Fig. 1a) that measures water vapor and carbon fluxes (since 2000), while in this region water is considered to be a valuable resource and the proper management of this resource depends on the accurate assessment of the ET component. Moreover, despite the well-known important contribution of drylands regions to global CO<sub>2</sub> (Ahlström et al., 2015), there are almost no efforts to estimate CO<sub>2</sub> fluxes in forested and non-forested areas in this dry region. This led to the development of the Weizmann mobile lab system (Israel; Fig. 1h), which allows the extension of the permanent FLUXNET measurement sites on campaign basis (e.g., Asaf et al., 2013; for technical detail see <http://www.weizmann.ac.il/EPS/Yakir/node/321>). Such a

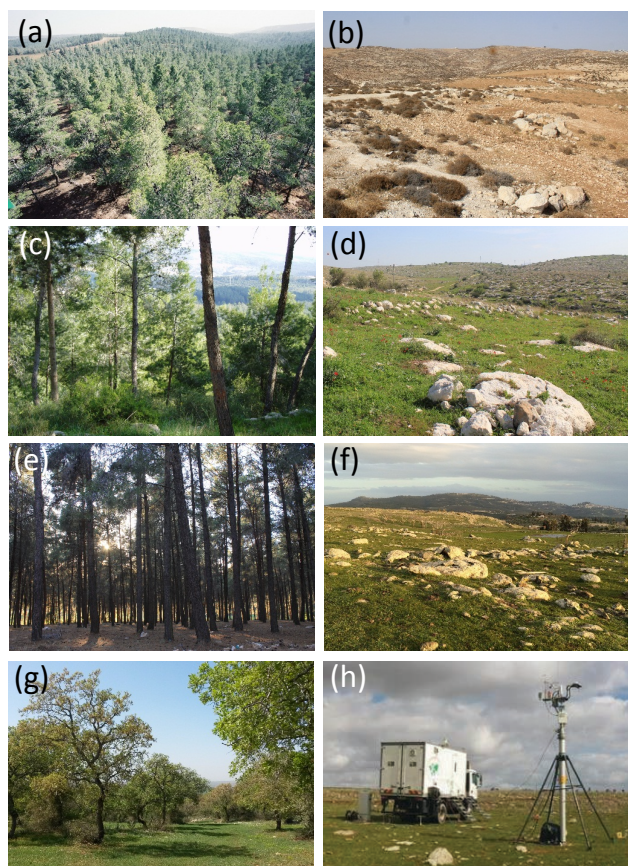


**Figure 1.** Views of the seven study sites along the climatic gradient (a–g) and the newly mobile flux measurement system used in this study (h). Sites include three paired planted pine forests (*Pinus halepensis*) and adjacent non-forest sites (representing the original environment in which these forests were planted): Yatir (a) and Wady Attir (b); Eshtaol (c) and Modiin (d); Biryá (e) and Kadita (f). The deciduous oak forest of HaSolelim is shown (g). The three paired sites (a–f) represent the geo-climatic transition from xeric to mesic environments in Israel.

system could allow flux and auxiliary analytical measurements across a range of climatic conditions, plant species and ecosystems, as well as addressing land use changes and disturbance. However, to extend these campaign-based measurements in time and space, a model fitted to the high-energy water-limited conditions of this region is required.

Here, we adjusted the RS–Met to the extreme hot and dry conditions of the eastern Mediterranean region. The adjusted RS–Met was examined in a total of seven ecosystems distributed at three precipitation levels along a rainfall gradient (280–770 mm yr<sup>−1</sup>) in this region (Israel; Fig. 1a–g). Ecosystems included three pairs of planted forests and adjacent non-forest sites (representing the original area in which these forests were planted). Ground-level campaign measurements of ET and net ecosystem CO<sub>2</sub> exchange using the newly developed mobile lab (Fig. 1h) and the continuous flux mea-

surements at the active FLUXNET site in Yatir (Klein et al., 2016; Tatarinov et al., 2016) were used to validate the RS–Met. This combination of model-based estimates and direct flux measurements of ET and CO<sub>2</sub> uptake across a range of climatic conditions and ecosystems provides a unique opportunity to test and validate the RS–Met approach in this high-energy water-limited region. Particularly, we examined the RS–Met with and without the application of the  $f_{WD}$ . We also compared the RS–Met with MODIS ET and GPP products at the studied sites.

Our specific goals in this study were to (1) examine the seasonal evolution of the  $f_{WD}$  and its role in the RS–Met; (2) compare the model estimates with EC and MODIS ET and GPP products across these high-energy water-limited sites, at a daily and annual basis; and (3) use the RS–Met to estimate changes in water use efficiency ( $WUE = GPP/ET$ ) following afforestation across the rainfall gradient in Israel, by comparing the three paired forest vs. non-forest sites.

## 2 Materials and methods

### 2.1 Study sites

The sites in this study included three pairs of planted pine forests (*Pinus halepensis* Mill.) and adjacent non-forested (dwarf shrublands) sites distributed throughout a climatic range in Israel ( $P = 280\text{--}770\text{ mm yr}^{-1}$ ), from dry to sub-humid Mediterranean (Table 1 and Fig. 1a–f), which represent the typical Mediterranean vegetation systems in the eastern Mediterranean. The three non-forested sites represent the original natural environment in which the pine forests were planted, while the afforested sites are currently managed by the Jewish National Fund (KKL). The non-forested shrubland sites are mostly dominated by *Sarcopoterium spinosum* (dwarf shrub) in a patchy distribution with a wide variety of herbaceous species, mostly annuals, growing in between the shrub patches during winter to early spring. In addition, we tested the models at one native deciduous forest site dominated by the *Quercus* species. A brief description of the sites is given in the following.

#### 2.1.1 Yatir

The forest of Yatir is an Aleppo pine forest (*Pinus halepensis*) that was planted by the KKL mostly during 1964–1969 in the semiarid region of Israel (31.34° N, 35.05° E; Fig. 1a). It covers a total area of ca. 2800 ha and lies on a predominantly light brown Rendzina soil ( $79 \pm 45.7\text{ cm}$  deep), overlying a chalk and limestone bedrock (Llusia et al., 2016). The average elevation is 650 m. The mean annual rainfall in the forest area is 285 mm yr<sup>−1</sup> (for the last 40 years) and was 279 mm yr<sup>−1</sup> at the FLUXNET site during 2001–2015 (Table 1). The mean annual temperature in Yatir is 18.2 °C with 13 and 31 °C for mean winter (November–January) and summer (May–July) temperatures, respectively. Tree den-

**Table 1.** Site characteristics and locations divided into two groups of forest (top) and non-forest (bottom) sites. In each group, sites are arranged from dry to humid (from top to bottom).

Site	Location (lat, N; long, E)	PFT	Dominant species	Grazing	Altitude	P	AF
Yatir	31.3451; 35.0519	CF	<i>P. halepensis</i>	sheep	660	279	0.19
Eshtaol	31.7953; 34.9954	CF	<i>P. halepensis</i>	sheep	385	480	0.34
HaSolelim	32.7464; 35.2317	OF	<i>Q. ithaburensis</i>	cattle	180	543	0.42
Birya	33.0015; 35.4823	CF	<i>P. halepensis</i>	cattle	750	766	0.63
Wady Attir	31.3308; 34.9905	SH	<i>Phagnalon rupestre</i>	sheep	490	279	0.11
Modiin	31.8698; 35.0125	SH	<i>S. spinosum</i>	cattle	245	480	0.32
Kadita	33.0110; 35.4614	SH	<i>S. spinosum</i>	cattle	815	766	0.63

PFT is the plant functional type (CF, coniferous forest; OF, oak forest; SH, shrubland); grazing indicates the main grazing regime at the site; altitude is in meters above sea level; *P* is the mean annual rainfall (mm yr<sup>-1</sup>); AF is the aridity factor calculated as the *P*-to-ET<sub>o</sub> ratio (mm mm<sup>-1</sup>).

sity in Yatir is ca. 300 trees ha<sup>-1</sup> (Rotenberg and Yakir, 2011) with a tree average height of ca. 10 m and canopy leaf area index (LAI) of  $1.4 \pm 0.4 \text{ m}^2 \text{ m}^{-2}$ , which displays small fluctuations between winter and summer (Sprintsin et al., 2011). The understory in this forest is mostly comprised of ephemeral herbaceous species (i.e., therophyte, geophytes and hemicryptophytes) growing during the wet season (September–April) and drying out in the beginning of the dry season (May–June). A relatively thin needle litter layer covers the forest floor during the needle senescence period (June–August; Maseyk et al., 2008).

### 2.1.2 Eshtaol

The forest of Eshtaol was planted in the late 1950s by the KKL with mostly *P. halepensis* trees in the central part of Israel (31.79° N, 34.99° E; Fig. 1c). The current forest area is ca. 1200 ha and lies mainly on Rendzina soils. The average elevation is 330 m. The mean annual rainfall in this area is ca. 500 mm yr<sup>-1</sup> and was a 480 mm yr<sup>-1</sup> at the site of the EC measurements during 2012–2015 (Table 1). Tree density in Eshtaol is typically 300–350 trees ha<sup>-1</sup>, with a tree canopy LAI that ranges between 1.9 and 2.6 m<sup>2</sup> m<sup>-2</sup> and a tree average height of 12.5 m (Osem et al., 2012).

### 2.1.3 Birya

The forest of Birya is a *P. halepensis* forest that was mostly planted during the early 1950s in the northern part of Israel in the Galilee region (33.00° N, 35.48° E; Fig. 1e). The forest covers an area of ca. 2100 ha and lies on Rendzina and Terra rossa soils. The average elevation is 730 m. The average temperature in this area is 16 °C, with an average annual rainfall of 710 and 776 mm yr<sup>-1</sup> during the years of the EC measurements (2012–2015; Table 1). The average stand density is 375 trees ha<sup>-1</sup> with an average tree height of 11 m (Llusia et al., 2016).

### 2.1.4 HaSolelim

The HaSolelim forest is a native deciduous mixed oak forest dominated by *Quercus ithaburensis*, which is accompanied by *Quercus calliprinos* (evergreen) and a few other Mediterranean broadleaved tree and shrub species (Fig. 1g). The forest is located in the northern part of Israel in the Galilee region, 30 km south of the Birya forest (32.74° N, 35.23° E). The forest covers an area of ca. 240 ha and lies on Rendzina and Terra rossa soils. The elevation at the site of the EC measurements is 180 m (Table 1). The average temperature in this area is typically 21 °C, with a mean annual rainfall of 580 mm yr<sup>-1</sup> and 543 mm yr<sup>-1</sup> during the years of the EC measurements. The site where the measurements took place is characterized by an average stand density of 280 trees ha<sup>-1</sup> and an average tree height of 8 m (Llusia et al., 2016).

### 2.1.5 Wady Attir

This is a xeric shrubland site located southwest from the forest of Yatir (31.33° N, 34.99° E). The average elevation is 490 m. The site is dominated by semi-shrub species, such as *Phagnalon rupestre* L. with *graminae* species, mainly *Stipa capensis* L. (also known as Mediterranean needle grass); *Hordeum spontaneum* K. Koc. (also known as wild barley); and some *Avena* species such as *A. barbata* L. and *A. sterilis* L., appearing shortly after the rainy season (Leu et al., 2014; Fig. 1b). The mean annual rainfall in this area is 230 mm yr<sup>-1</sup> (Mussery et al., 2016) and was 280 mm yr<sup>-1</sup> in the years of the EC measurements (2012–2015; Table 1).

### 2.1.6 Modiin

The shrubland site of Modiin is located a few kilometers from the forest site of Eshtaol and represents the original environment in which this forest was planted (31.87° N, 35.01° E; Fig. 1d). The average elevation is 245 m. The shrubland site is mostly dominated by *Sarcopoterium spinosum* (dwarf shrub) in a patchy distribution with a wide variety of herbaceous species, mostly annuals, growing in be-

tween the shrub patches from winter to early spring. The average rainfall amount in this area was 480 mm yr<sup>-1</sup> in the years of the EC measurements (Table 1).

### 2.1.7 Kadita

The shrubland site of Kadita is also dominated by *Sarcopoterium spinosum* (dwarf shrub) in a typical patchy distribution (Fig. 1f). It is located near the forest of Biryá at an elevation of 815 m (33.01° N, 35.46° E; Table 1). The mean annual rainfall at this site is similar to that recorded in the Biryá forest (i.e., 766 mm yr<sup>-1</sup> in the years of study).

All shrubland sites have been under continuous livestock grazing for many years, and their vegetation structures are mainly the outcome of both rainfall amount and grazing regime.

## 2.2 Satellite-derived vegetation index

We used the NDVI from the MODIS onboard NASA's Terra satellite at 250 m spatial resolution (MOD13Q1). The MOD13Q1 NDVI product is a composite of a single day's value selected from 16-day periods based on the maximum value criteria (Huete et al., 2002). Terra's NDVI product is acquired during the morning (10:30 LT) and thus provides a good representation of the peak time of the plants' diurnal activity. The gradual growth of the vegetation enables the interpolation of the 16-day NDVI time series to representative daily values (Glenn et al., 2008; Maselli et al., 2014). We downloaded the 16-day NDVI time series covering the main area of the EC flux measurement for each site from the MODIS subsets ([http://daacmodis.ornl.gov/cgi-bin/MODIS/GLBVIZ\\_1\\_Glb/modis\\_subset\\_order\\_global\\_col5.pl](http://daacmodis.ornl.gov/cgi-bin/MODIS/GLBVIZ_1_Glb/modis_subset_order_global_col5.pl)) for the period October 2001–October 2015. Then we preprocessed the NDVI time series as described in Helman et al. (2014a, b, 2015b) to remove outliers and uncertainties due to cloud contamination and atmospheric disturbances without removing important information (see Fig. S2 in the Supplement). The processed 16-day NDVI time series were then interpolated on a daily basis using the local scatter plot smoothing technique (LOESS). This technique is suited for eliminating outliers in non-parametric time series and has been shown to be a useful tool in the interpolation of datasets with a seasonal component (Cleveland, 1979).

## 2.3 The mobile lab system and the FLUXNET station in Yatir

A newly designed mobile flux measurement system was used in all campaigns (Fig. 1h), based on the 28 m pneumatic mast on a 12 tons 4 × 4 truck that included a laboratory providing an air-conditioned instrument facility (cellular communication, 18 kVA generator, 4200 W UPS). Flux, meteorological and radiation measurements relied on an EC system that provides CO<sub>2</sub> measurements and sensible and latent heat fluxes using a three-dimensional sonic anemometer (R3,

Gill Instruments, Lymington, Hampshire, UK) and enclosed-path CO<sub>2</sub>–H<sub>2</sub>O infrared gas analyzer (IRGA) (Licor 7200, Li-Cor, Lincoln, NE, USA) using CARBOEUROFLUX methodology (Aubinet et al., 2000), and EddyPro software ([www.licor.com](http://www.licor.com)). Data were collected using a self-designed program in LabVIEW software. Air temperature and relative humidity (HMP45C probes, Campbell Scientific) and air pressure (Campbell Scientific sensors) were measured at 3 m above the canopy. Energy fluxes relied on radiation sensors, including solar radiation (CMP21, Kipp and Zonen), long-wave radiation (CRG4, Kipp and Zonen) and photosynthetic radiation (PAR, PAR-LITE2) sensors. All sensors were installed in pairs facing both up and down and were connected using the differential mode through a multiplexer to a data logger (Campbell Scientific). GPP for each site was calculated from the measured net ecosystem CO<sub>2</sub> exchange (NEE) after estimating ecosystem respiration, Re, and using the regression of NEE on turbulent nights against temperature, followed by extrapolating the relationship that was found between Re and temperature during the nighttime and daytime periods (Reichstein et al., 2005; modified for our region by Afik, 2009). Flux measurements with the mobile system were carried out on a campaign basis, at six of the seven sites, with each campaign representing approximately 2 weeks at a single site, repeated along the seasonal cycle with mostly two but sometimes only one 2-week sets of measurements per cycle, during the 4 years of measurements, 2012–2015. Continuous flux measurements were carried out at the permanent FLUXNET site of Yatir (xeric forest site). Began in 2000, the EC and supplementary meteorological measurements have been conducted continuously (Rotenberg and Yakir, 2011; Tatarinov et al., 2016), with measurements performed according to the EUROFLUX methodology. Instrumentation is similar to that in the mobile lab except for the use of a closed-path CO<sub>2</sub>–H<sub>2</sub>O IRGA (LI-7000; Li-Cor, Lincoln, NE) with the inlet placed 18.7 m above the ground. Typical fetch providing 70 % (cumulative) contribution to turbulent fluxes was measured between 100 and 250 m (depending on the site) along the wind distance. This was taken into consideration when using the MOD13Q1 product to derive the modeled fluxes.

During April 2012, at the peak activity season in Yatir forest, for 2 weeks the mobile lab system was deployed 10 m away from the permanent flux measurement tower, where both EC systems were measuring at the same height and fluxes were calculated by the same software (EddyPro 3.0 version; Li-Cor, USA). The linear correlation ( $R^2$ ) and the slope of the mobile lab vs. the FLUXNET tower was 0.9 and 1.0 for the sensible heat, 0.8 and 0.9 for latent heat, and 0.9 and 1 for the NEE, respectively.

Daily estimates of reference evapotranspiration, i.e., ET<sub>o</sub> (mm d<sup>-1</sup>), for the ET model, the water deficit and the water availability factors were calculated from the mean daily air temperature and the daily total incoming solar radiation, measured at the seven sites following the empirical formula-



tion proposed by Jensen and Haise (1963):

$$ET_o = \frac{R_g}{2470} (0.078 + 0.0252T), \quad (1)$$

in which  $T$  is the mean daily air temperature (°C), and  $R_g$  is the daily global (total) incoming solar radiation ( $\text{kJ m}^{-2} \text{d}^{-1}$ );  $ET_o$  is finally converted into millimeters per day by dividing the  $R_g$  by  $2470 \text{ mm kJ m}^{-2} \text{d}^{-1}$  (see in Jensen and Haise, 1963). We decided to use this  $ET_o$  formulation of Jensen and Haise (1963) to be consistent with the original RS–Met proposed by Maselli et al. (2014), though we are aware of the large tradition of works devoted to comparing several methods to estimate  $ET_o$  and to proving the validity and limitations of these methods under different environmental conditions.

## 2.4 MODIS ET and GPP products and the PaVI-E model for annual ET

We compared our RS–Met with the products from MODIS-based ET and GPP models, the details of which can be found in Mu et al. (2007, 2011) and Running et al. (2000, 2004) for the ET and GPP models, respectively. These products (MOD16 and MOD17 for ET and GPP, respectively) provide 8-day ET and GPP estimates at 1 km for 2000–2015, globally. MODIS ET and GPP products were compared with RS–Met on seasonal and annual scales at all sites. Importantly, these MODIS products take advantage of the use of vapor pressure information, which was shown to affect the stomatal conductance of plants, whereas our model did not consider this factor directly. We did not use vapor pressure data in the RS–Met because most of the weather stations in this region do not have such information and that would have limited the use of our model. However, the  $f_{WD}$  calculated from radiation, temperature and water supply (rainfall) data is used in the adjusted RS–Met as an indirect proxy for vapor pressure deficit (VPD). To compare with the 8-day MODIS ET and GPP products we averaged the daily RS–Met and EC estimates over the same 8-day periods.

We also compared the RS–Met ET estimates to the annual ET derived from PaVI-E (parameterization of vegetation index for the estimation of the ET model; Helman et al., 2015a), at the six sites on an annual basis. The PaVI-E is an empirical model based on simple exponential relationships found between MODIS-derived enhanced vegetation index (EVI) and NDVI and annual ET estimates from EC at 16 FLUXNET sites, comprising a wide range of plant functional types across Mediterranean climate regions. This simple relationship (PaVI-E) was shown to produce accurate ET estimates on an annual timescale ( $\text{mm yr}^{-1}$ ) and at a moderate spatial resolution of 250 m in this region (Helman et al., 2015a). It was validated against physical-based models (MOD16 and the Land Surface Analysis Satellite Applications Facility (LSA-SAF) product of ET) and ET calculated from water balances across the same study area. PaVI-E was

used for ecohydrological studies in this region, providing insights into the role of climate in altering forest water and carbon cycles (Helman et al., 2017a, b). The advantage of this model is that it does not require any additional meteorological information but is a proper function of the relationship between observed fluxes and satellite-derived vegetation indices. This makes it interesting to compare with the RS–Met model since the RS–Met is highly dependent on meteorological forcing.

## 3 Description of the models and the use of a water deficit factor

The RS–Met models used here for the daily estimation of ET and GPP are based on the NDVI and the meteorological data. Each model was applied with and without a water deficit factor ( $f_{WD}$ ) adjustment (i.e., two model versions for ET and two for the GPP).

### 3.1 The ET model

The RS–Met of daily ET is based on the FAO-56 formulation (Eq. 2):

$$ET = ET_o \times (K_C + K_S), \quad (2)$$

in which  $K_C$  and  $K_S$  stand for the canopy and soil coefficients, respectively (Allen et al., 1998). In the RS–Met a maximum value of  $K_C$  ( $K_{C\_max}$ ), which depends on the type of the monitored vegetation (Allen et al., 1998, 2006), and a maximum value of  $K_S$  ( $K_{S\_max}$ ), for soil evaporation, are used as a reference in the model.  $K_{C\_max}$  and  $K_{S\_max}$  are then multiplied by a linear transformation of the NDVI (i.e.,  $f(\text{NDVI})$  and  $f(1-\text{NDVI})$ , respectively; Maselli et al., 2014) to adjust for the seasonal evolution of the canopy and soil coefficients:

$$K_C = K_{C\_max} \times f(\text{NDVI}) \quad (3)$$

$$K_S = K_{S\_max} \times f(1 - \text{NDVI}). \quad (4)$$

The linear transformation of the NDVI used here is the fractional vegetation cover ( $fVC$ ) that better represents both ET processes: direct soil evaporation and plant transpiration. The  $fVC$  is a classical two-end member function based on minimum and maximum values of NDVI, corresponding to a typical soil background without vegetation ( $\text{NDVI}_{\text{SOIL}}$ ) and an area fully covered by vegetation ( $\text{NDVI}_{\text{VEG}}$ ):

$$fVC = (\text{NDVI} - \text{NDVI}_{\text{SOIL}}) / (\text{NDVI}_{\text{VEG}} - \text{NDVI}_{\text{SOIL}}). \quad (5)$$

Thus, Eqs. (3) and (4) become

$$K_C = K_{C\_max} \times fVC \quad (6)$$

and

$$K_S = K_{S\_max} \times (1 - fVC), \quad (7)$$

respectively.

The  $fVC$  in Eq. (5) is calculated on a daily basis from the interpolated NDVI (daily) data. Note that the  $fVC$  in Eq. (6) represents the fraction of the area covered by the vegetation, while in Eq. (7) the term  $1-fVC$  represents the fraction of the bare soil area. Both terms,  $fVC$  and  $1-fVC$ , in Eqs. (6) and (7), change over the course of a year due to canopy development and/or the appearance of ephemeral herbaceous plants. Here we used the values of 0.1 and 0.8 for the  $NDVI_{SOIL}$  and  $NDVI_{VEG}$ , respectively, which are the values observed for bare ground and dense natural vegetation in this region (Helman et al., 2015b).

Finally, from Eqs. (2) and (5)–(7) we obtain the model without the water deficit factor adjustment (NO  $f_{WD}$ ):

$$ET = ET_o \times \{[fVC \times K_{C\_max}] + [(1 - fVC) \times K_{S\_max}]\}. \quad (8)$$

Subsequently, we used water deficit ( $f_{WD}$ ) and water availability ( $f_{WA}$ ) factors to adjust the canopy and soil coefficients for water supply conditions in the root zone and top soil in Eqs. (6) and (7), respectively:

$$K_C = K_{C\_max} \times fVC \times f_{WD} \quad (9)$$

and

$$K_S = K_{S\_max} \times (1 - fVC) \times f_{WA}. \quad (10)$$

The  $f_{WD}$  and  $f_{WA}$  in Eqs. (9) and (10) simulate the effects of available water for plant transpiration in the root zone and for surface evaporation in the top soil, respectively, whereas the  $f_{WD}$  is defined as follows:

$$f_{WD} = 0.5 + 0.5 \times f_{WA}. \quad (11)$$

The water availability factor ( $f_{WA}$ ) is calculated as the simple ratio between the daily rainfall amount and the daily  $ET_o$ , both cumulated over a period of 2 months. Basically, the accumulation period could vary for different ecosystem types and environmental conditions. However, we have taken a period of 2 months for the native shrublands and planted (and native) forests following previous observations that showed that this period is sufficient to maintain the wet topsoil layer for the whole rainy season in ecosystems in this region (Raz-Yaseef et al., 2012). Furthermore, changing the accumulation period did not give us consistently better results at all sites, as the 2-month period gave us.

The  $f_{WA}$  is set to 1 when the cumulated rainfall amount exceeds the atmospheric demand (i.e., the  $ET_o$ ). Note that the  $f_{WD}$  would then vary between 0.5 and 1, meaning that  $ET$  is reduced to half the potential maximum in the absence of water supply, simulating the basic transpiration levels maintained by evergreen vegetation (Glenn et al., 2011; Maselli et al., 2014). This reduction in the  $f_{WD}$  accounts for water deficit in the root zone, which results in reduced plant

transpiration, while short-term effects would be mainly reflected through changes in the NDVI (and consequently in the  $fVC$  and  $fAPAR$ ; Glenn et al., 2010; Running and Nemani, 1988). In contrast to the  $f_{WD}$ , the  $f_{WA}$  is reduced to zero following a dry period longer than 2 months, making the surface evaporation component null during the dry summer.

The model is adjusted to root zone and surface water deficit conditions ( $f_{WD}$  and  $f_{WA}$ ) by replacing Eqs. (6) and (7) with Eqs. (9) and (10):

$$ET = ET_o \times \{[fVC \times K_{C\_max} \times f_{WD}] + [(1 - fVC) \times K_{S\_max} \times f_{WA}]\}. \quad (12)$$

Here we used a  $K_{C\_max}$  value of 0.7 for both forests and non-forest sites, and we used a  $K_{S\_max}$  value of 0.2 for soil evaporation in both (adjusted and unadjusted for water deficit conditions) models, as in Maselli et al. (2014).

Finally, the model derives daily  $ET$  estimates ( $\text{mm d}^{-1}$ ) at the spatial resolution of the MODIS NDVI product, i.e., 250 m.

### 3.2 The GPP model

For the GPP model, we used the biophysical radiation use efficiency model proposed by Monteith (1977):

$$GPP = RUE \times fAPAR \times PAR, \quad (13)$$

in which  $PAR$  is the daily incident photosynthetic active radiation ( $\text{MJ m}^{-2}$ ), calculated as 45.7 % from the incoming measured global solar radiation (Nagaraja Rao, 1984), and  $fAPAR$  is the fraction of the  $PAR$  that is actually absorbed by the canopy (range from 0 to 1). The  $fAPAR$  was derived here from the daily NDVI time series following the linear formulation:  $fAPAR = 1.1638 \text{ NDVI} - 0.1426$ , which was proposed by Myneni and Williams (1994). This linear formulation was successfully applied in similar remote-sensing-based GPP models for similar ecosystems by Veroustraete et al. (2002), Maselli et al. (2006, 2009) and Helman et al. (2017a);  $RUE$  is the radiation use efficiency ( $\text{g C MJ}^{-1}$ ), which is the efficiency of the plant for converting the absorbed radiation into carbon-based compounds and which changes over the course of a year (Garbulsky et al., 2008).

The  $RUE$  is an important component in the GPP model and is the most challenging parameter to compute. It is usually considered to be related to VPD, water availability, temperature and plant species type (Running et al., 2000), and there have been several recent efforts to directly relate it to the photochemical reflectance index (PRI), which can also be derived from satellites (Garbulsky et al., 2014; Peñuelas et al., 2011; Wu et al., 2015). Currently, the conventional modeling of  $RUE$  for Mediterranean ecosystems is not straightforward and is mostly site specific, derived for specific local conditions (Garbulsky et al., 2008). Here, we used the simple approach proposed by Veroustraete et al. (2002) and further developed by Maselli et al. (2009), which states that a

potential RUE (RUE<sub>MAX</sub> in g C MJ<sup>-1</sup>) can be adjusted for seasonal changes using a function based on temperature and water deficit conditions ( $f_{WT}$ ):

$$RUE = RUE_{MAX} \times f_{WT}. \quad (14)$$

The  $f_{WT}$  adjusts the RUE<sub>MAX</sub> for seasonal changes following changes in water availability and temperature conditions:

$$f_{WT} = T_{CORR} \times f_{WD}, \quad (15)$$

in which  $T_{CORR}$  is a temperature correction factor calculated on a daily basis (Veroustraete et al., 2002):

$$T_{CORR} = \frac{e\left(a - \frac{\Delta H_{AP}}{G \cdot T}\right)}{1 + e\left(\frac{\Delta S \cdot T - \Delta H_{DP}}{G \cdot T}\right)}, \quad (16)$$

in which  $a$  is a constant equal to 21.9;  $\Delta H_{AP}$  and  $\Delta H_{DP}$  are the activation and deactivation energies (J mol<sup>-1</sup>), equal to 52 750 and 211, respectively;  $G$  is the gas constant, equal to 8.31 J K<sup>-1</sup> mol<sup>-1</sup>;  $\Delta S$  is the entropy of the denaturation of CO<sub>2</sub> and is equal to 710 J K<sup>-1</sup> mol<sup>-1</sup>;  $T$  is the mean daily air temperature (in degrees Kelvin); and  $f_{WD}$  is the same water deficit factor as in Eq. (11).

The water deficit factor,  $f_{WD}$ , is used here only in the model that considers water supply conditions. Thus, in the model without the  $f_{WD}$ , the  $f_{WT}$  would be only a function of the temperature, and thus  $f_{WT} = T_{CORR}$  (in Eq. 15). Following Garbulsky et al. (2008) and Maselli et al. (2009), a constant value of 1.4 g C MJ<sup>-1</sup> was used here for RUE<sub>MAX</sub> at all sites and in model variations (i.e., with and without the  $f_{WD}$ ). The exclusion of direct measurements of VPD as an input in the model is indeed a limitation; however, we tried to maintain a model with minimal input data that will be available from standard weather stations (VPD information is currently lacking from most of the weather stations in this region). The inclusion of the  $f_{WD}$ , which includes radiation, temperature and water supply (rainfall) information, is used as an indirect proxy for VPD in the model.

Finally, daily GPP values were computed from the model at a spatial resolution of 250 m for each of the seven sites and compared with EC estimates and the MODIS GPP product. It should be stated that the use of the EC-derived GPP as a reference in the validation should be taken with caution because GPP by itself is modeled and not directly measured. This may introduce uncertainties in the validation that could be contaminated by self-correlation.

#### 4 Testing the water deficit factor in high-energy water-limited environments

To show the importance of the water deficit factor ( $f_{WD}$ ) in adjusting the model to seasonal variations in the fluxes, we demonstrate the seasonal evolution of the  $f_{WD}$  together with that of the main drivers of the RS–Met at the dryland pine

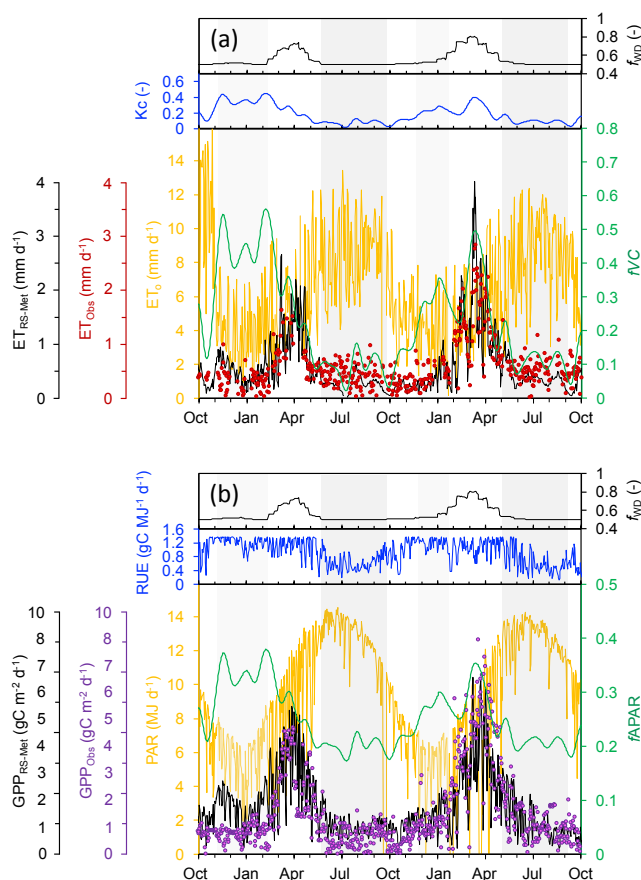


**Figure 2.** Seasonal evolution of the water deficit factor ( $f_{WD}$ ; black line in upper panel) and the main drivers of the modeled ET (a) and GPP (b) in the semiarid pine forest of Yatir (ET<sub>RS–Met</sub> and GPP<sub>RS–Met</sub>, respectively; black line in lower panel) for the seasonal years 2008/09 and 2009/10. EC fluxes are also shown (ET<sub>Obs</sub> and GPP<sub>Obs</sub>, red and purple dots, respectively). The  $K_C$  and the radiation use efficiency (RUE) both without the addition of the  $f_{WD}$  (blue in middle panels) are shown together with the potential ET (ET<sub>O</sub>, yellow in a), the fraction of vegetation cover ( $f_{VC}$ , green in a), the photosynthetic active radiation (PAR, yellow in b) and the fraction of absorbed PAR ( $f_{APAR}$ , green in b). Colored vertical bands indicate the critical periods when the addition of  $f_{WD}$  is particularly useful.

forest site of Yatir (Fig. 2). Figure 2a shows that the  $f_{WD}$  moderates the increase in  $K_C$  (blue line in middle panel of Fig. 2a) at the beginning of the rainy season (November–January) even though the  $f_{VC}$  (green line in lower panel of Fig. 2a) is relatively high, likely due to the appearance of ephemeral herbaceous vegetation in the forest understory (Helman et al., 2015b). This is a realistic scheme since the herbaceous vegetation has little contribution to the ecosystem fluxes but a significant contribution to the NDVI (and thus to the  $f_{VC}$ ) signal (Helman, 2017), as observed by the low EC GPP at this time (red dots in lower panel of Fig. 2a). Thus, the  $f_{WD}$  has an important role in reducing the  $K_C$  to



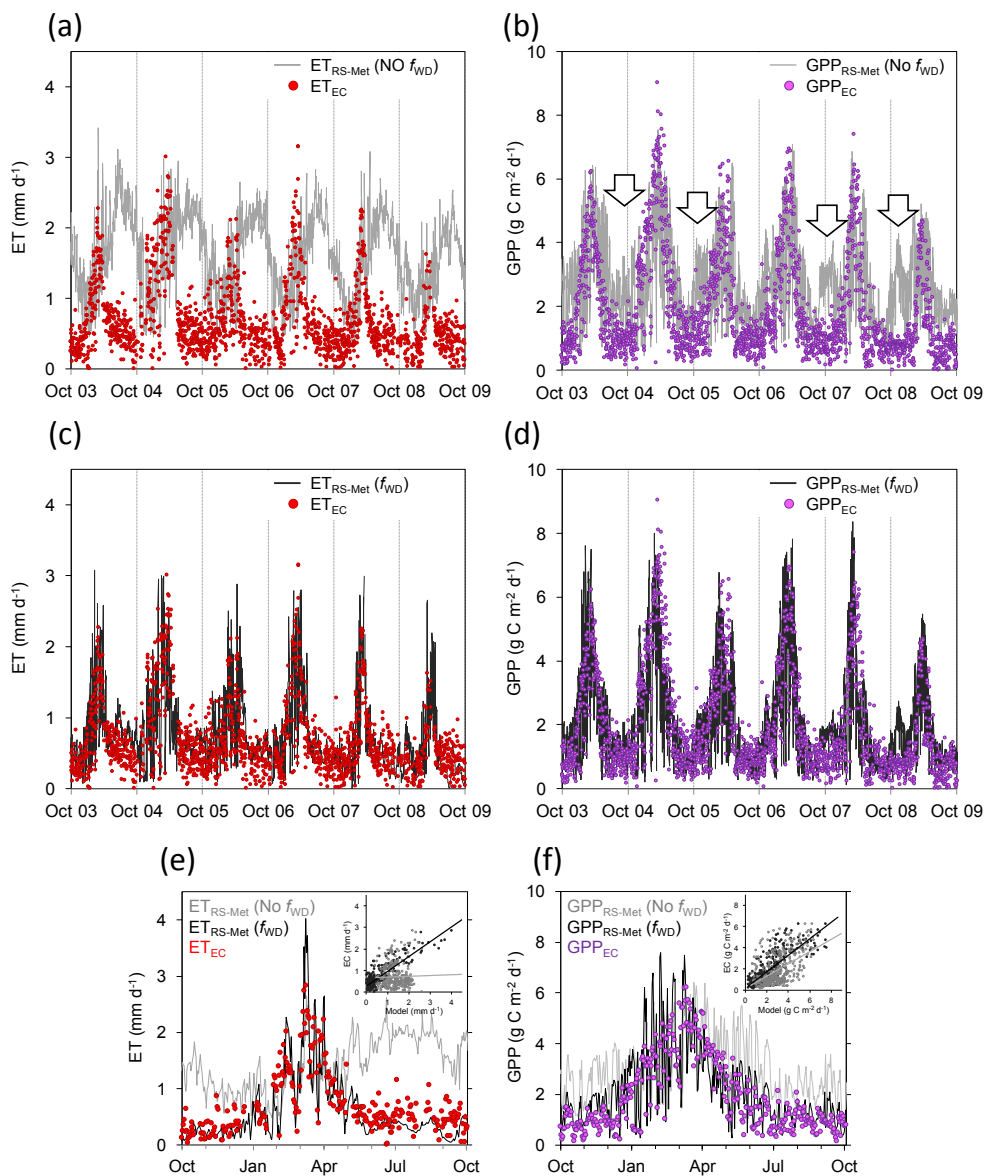


**Figure 3.** Observed (EC) and modeled (RS–Met) ET and GPP at Yatir. Shown in (a)–(d) are the RS–Met values with (black) and without (grey) the water deficit factor ( $f_{WD}$ ). A closer look at the selected years 2009/10 and 2003/04 is shown in (e) and (f), respectively. Inserts show the correlations between modeled and observed fluxes with and without the  $f_{WD}$  (black and grey dots, respectively).

more realistic low values at this stage of the year when there is less water available for the trees. The same applies for the end of the rainy season and summer, in May–August, when the  $ET_o$  is relatively high but there is almost no available water for ET, as implied from the low  $f_{WD}$  (black line in upper panel of Fig. 2a).

In the GPP model, the  $f_{WD}$  reduces the high RUE at both ends of the rainy season, adjusting the GPP to the water deficit conditions in the root zone during these periods (Fig. 2b). Here again, the low  $f_{WD}$  reduces the contribution of the high  $f_{APAR}$  (and the RUE) in the model during the start of the rainy season due to the growth of ephemeral

plants in the understory (green and blue lines in lower and middle panels of Fig. 2b, respectively). This is because there is still not sufficient water in the root zone during this period. Particularly noted, though, is the significant reduction in GPP at the end of the rainy season and during the summer (May–August), when the PAR (yellow line in lower panel of Fig. 2b) is high but less water is available for transpiration and subsequently for photosynthesis.

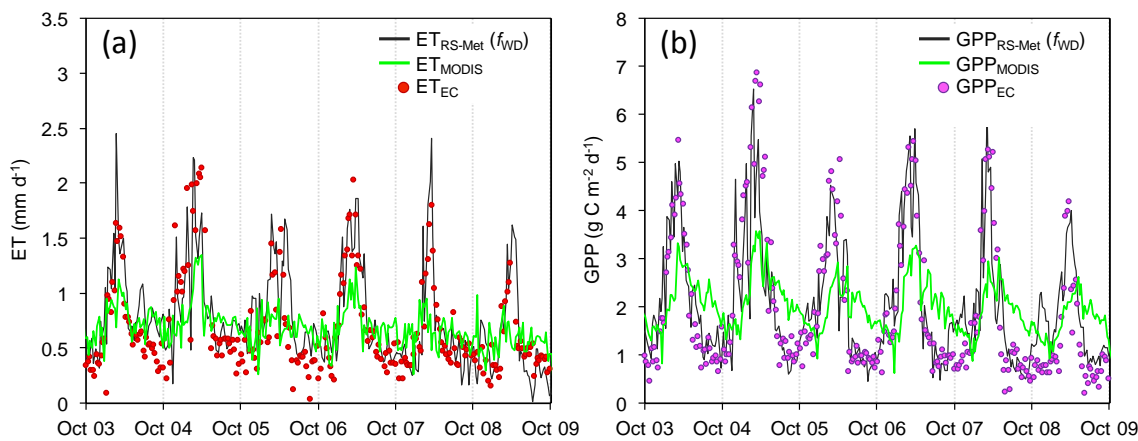


**Figure 4.** Showing 8-day averaged values of ET (a) and GPP (b) from EC (dots), RS–Met (black) and MODIS (green) at Yatir. The  $R$  of the correlation for EC vs. RS–Met is 0.78 and 0.80 for ET and GPP, respectively (slope = 0.90 and 0.70; intercept = 0.19 and 0.66 for ET and GPP, respectively). The  $R$  of the correlation for EC vs. MODIS is 0.47 and 0.60 for ET and GPP, respectively (slope = 0.21 and 0.27; intercept = 0.56 and 1.47 for ET and GPP, respectively).

**Table 2.** Statistics of the comparison between the RS–Met with the addition of the water deficit factor ( $f_{WD}$ ) and without its addition (NO  $f_{WD}$ ) and the EC-derived measurements.

	ET (mm d <sup>−1</sup> )						GPP (g C m <sup>−1</sup> d <sup>−1</sup> )					
	N	Correlation		MAE			N	Correlation		MAE		
		NO $f_{WD}$	$f_{WD}$	NO $f_{WD}$	$f_{WD}$			NO $f_{WD}$	$f_{WD}$	NO $f_{WD}$	$f_{WD}$	
Yatir	2228	0.05*	0.76	1.9	0.18		2293	0.56	0.77	1.3	0.8	
Eshtaol	47	0.16 <sup>ns</sup>	0.64	1.3	1.6		54	0.80	0.90	2.3	2.3	
HaSolelim	40	0.72	0.79	2.0	0.8		41	0.80	0.88	2.1	2.1	
Birya	57	0.72	0.85	1.8	1.8		57	0.64	0.72	4	3	
Wady Attir	28	0.80	0.91	0.5	0.7		29	0.90	0.92	0.7	1.0	
Modiin	43	0.62	0.64	1.9	1.0		43	0.89	0.90	1.2	1.2	
Kadita	28	0.80	0.67	0.8	1.0		28	0.82	0.88	1.8	1.8	

The mean absolute error (MAE) is in mm d<sup>−1</sup> for the ET and in g C m<sup>−2</sup> d<sup>−1</sup> for the GPP. All the correlations were highly statistically significant at  $P < 0.001$ , except for the ET model without the  $f_{WD}$  at the forest site of Yatir (\*), which was significant at  $P = 0.02$ , and the site of Eshtaol, which was not statistically significant (ns). The number of days used for the correlation at each site and flux is indicated ( $N = \text{days}$ ).

## 5 Comparisons with MODIS and the FLUXNET station in Yatir

### 5.1 Daily ET and GPP

We compared the daily estimates of the modeled ET with MODIS ET and GPP products and the active FLUXNET station at the dryland pine forest of Yatir for 2002–2012 (Table 1). As expected from the information noted above (Sect. 4), the model without the water deficit factor (NO  $f_{WD}$  in Fig. 3a and e) overestimated the ET in comparison to the EC measurements, particularly from mid-spring to the end of the summer (Fig. 3a, e). The peak ET was shifted to late July–early September, while the ET measured from the EC showed an earlier peak, in March. The large overestimation of the model without the  $f_{WD}$  was associated with the high  $ET_o$  during the spring and summer ( $R = 0.91$ ;  $P < 0.001$ ; see

also Fig. 2a), which is the driver of the ET model (Eqs. 2, 8 and 12), following the low humidity and augmented radiation load at this time of the year (Fig. 2 and Rotenberg and Yakir, 2011; Tatarinov et al., 2016). However, including the  $f_{WD}$  in the model helped to correct for this overestimation by linking ET to the available soil water (Fig. 2a), resulting in a good agreement between the model and the EC estimates (Fig. 3c and e; Table 2).

When comparing the modeled GPP with the EC estimates at Yatir, the model without the  $f_{WD}$  (NO  $f_{WD}$  in Fig. 3b and f) produced higher values during both ends of the rainy season (October–November and May–June). In particular, the model without the  $f_{WD}$  overestimated the GPP during the start of the rainy season (indicated by the arrows in Fig. 3b). This was likely due to the increase in the NDVI following the appearance of ephemeral herbaceous plants in the understory of these Mediterranean forests in the beginning of the

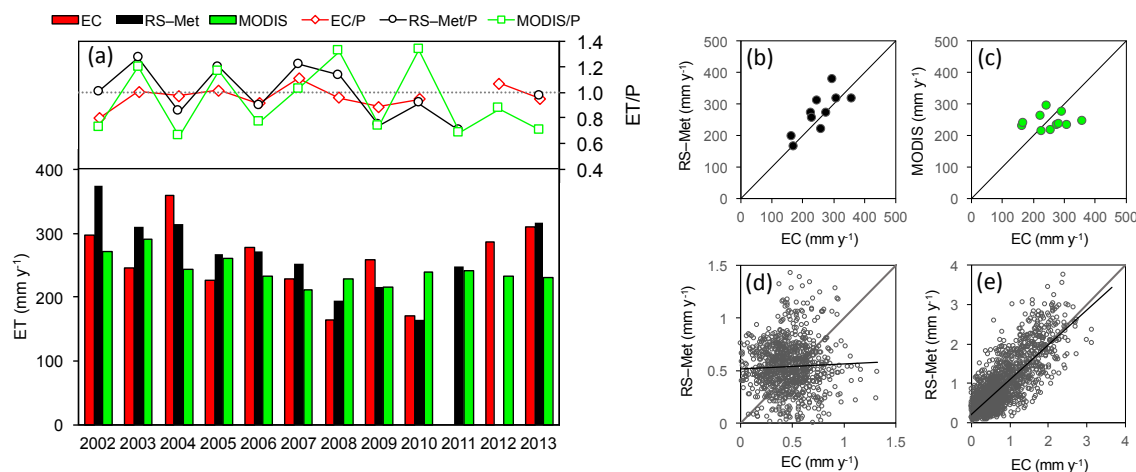


**Figure 5.** Annual ET ( $\text{mm yr}^{-1}$ ) summed from daily RS–Met (with  $f_{\text{WD}}$ , black), MODIS (green) and EC (red) at the Yatir forest site for 2003–2014 (a). Linear regressions of the EC vs. RS–Met (b) and EC vs. MODIS (c). Daily estimates from RS–Met in dry summer (June–August, d) and rainy (October–May, e) seasons. The  $R$ 's of the linear fits for EC vs. RS–Met (b) and MODIS (c) are 0.78 ( $P < 0.05$ ,  $N = 10$ ) and 0.10 ( $P > 0.1$ ,  $N = 11$ ), respectively. The  $R$ 's of the linear fits for the daily data in (d) and (e) are 0.05 ( $P > 0.1$ ,  $N = 876$ ) and 0.80 ( $P < 0.0001$ ,  $N = 1570$ ), respectively. The interannual trends in ET /  $P$  from EC, RS–Met and MODIS are presented in the upper panel of (a). Note that the annual sums of ET from EC and RS–Met in 2011 and 2012, respectively, are not displayed due to the scarcity of available data during these years ( $> 50\%$  missing data).

rainy season, as already pointed out in the previous section (see also Helman et al., 2015b). The herbaceous vegetation in the understory of Yatir provides a meaningful contribution to the NDVI signal, although it constitutes only a minor component in terms of the biomass and the CO<sub>2</sub> uptake of the forest (Helman et al., 2015b; Rotenberg and Yakir, 2011). Considering  $f_{\text{WD}}$  in the model thus abridged the RUE, counterbalancing the high contribution of the herbaceous vegetation to the  $f_{\text{APAR}}$  through the high NDVI. This also better simulated the water deficit conditions experienced by the woody vegetation, which is the main contributor to the GPP in Yatir during the dry period (Fig. 3d and f).

These results explicitly show that the water deficit factor is useful in forcing the model onto the woody vegetation activities (strongly restricted by water shortage at both ends of the rainy season), reducing the impact of other components, such as the peak activities of the understory vegetation that, obviously, does not suffer from water shortage and responds to a small early season moisture input (Helman et al., 2014a, 2017c; Musser et al., 2016).

Comparison with MODIS ET and GPP products shows a consistent underestimation of the fluxes in the peak season and overestimation in the dry season, implying that these models need to be adjusted to root-zone water deficit conditions at such high-energy water-limited sites (Fig. 4). This is in spite of the use of vapor pressure data in these models (Mu et al., 2007, 2011; Running et al., 2000, 2004). These results suggest that including the  $f_{\text{WD}}$  in global models, such as the MODIS-based models, might at least reduce the ob-

served dry period overestimations and increase fluxes in the wet season.

## 5.2 Annual-basis comparisons

We then examined the adjusted RS–Met on an annual scale, first by comparing the inter-annual variation in the modeled ET with that from the EC and with that from the MODIS ET product at Yatir (Fig. 5a). This analysis indicated that RS–Met can also reproduce the annual ET with a fair accuracy, showing a moderate but significant correlation with the total annual ET derived from the daily summed EC estimates ( $R = 0.78$ ;  $P < 0.05$ ;  $N = 10$ ; Fig. 5b) and comparable mean annual ET ( $266 \pm 61$  vs.  $257 \pm 58 \text{ mm yr}^{-1}$  for  $\text{ET}_{\text{MOD}}$  and  $\text{ET}_{\text{EC}}$ , respectively). MODIS ET, in turn, was not correlated with EC ( $R = 0.10$ ;  $P > 0.1$ ;  $N = 11$ ), showing little year-to-year variation in the annual ET (Fig. 5a, c).

Both the RS–Met and the EC were significantly correlated with  $P$  ( $R = 0.60$  and  $0.93$ ;  $P = 0.05$  and  $< 0.001$ ), showing similar patterns in water use (ET /  $P$  ratio), though differing in magnitude in some of the years studied (black and red lines in upper panel of Figs. 5a and S3). The little year-to-year variation in the MODIS ET resulted in a noisier pattern of water use (green line in upper panel of Fig. 5a) compared to that calculated from the RS–Met and EC. A noisy water use pattern was also noted in the RS–Met (compared to that from the EC), particularly in dry years (Fig. S3; e.g., 2003, 2005 and 2008; Fig. 5a). Higher ET in the RS–Met was likely the result of discrepancies in daily estimates during the summer between the RS–Met and EC ( $R = 0.05$ ,  $P > 0.1$  for June–August; Fig. 5d). This is supported by the observation of a

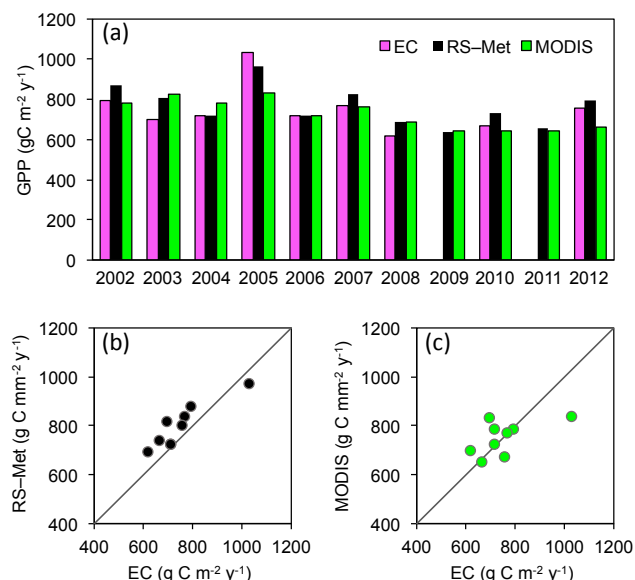


**Figure 6.** Annual GPP sums (gC m<sup>-2</sup> yr<sup>-1</sup>) from EC, RS-Met (with  $f_{WD}$ ) and the 8-day MOD16 product (MODIS) at Yatir (a) and the linear regressions of EC vs. RS-Met (b) and MODIS (c). The  $R$  of the linear fits is 0.91 ( $P < 0.05$ ,  $N = 10$ ) and 0.58 ( $P = 0.08$ ,  $N = 10$ ) for RS-Met and MODIS, respectively. Annual EC GPP for 2009 and 2011 was not calculated due to missing data.

5-fold higher bias between EC and RS-Met summer daily estimates in those dry years (bias =  $-0.146$  mm d<sup>-1</sup>), compared to the remaining years (bias =  $-0.029$  mm d<sup>-1</sup>). These negative biases imply an average overestimation by the RS-Met model during the summer compared to observed (EC) ET estimates.

In contrast, the correlation between the RS-Met and EC was high and significant for daily estimates during the rainy season ( $R = 0.80$ ,  $P < 0.0001$  for October–May; Fig. 5e). The relatively large discrepancies between RS-Met and EC during the summer indicate the low sensitivity of the RS-Met model to relatively low ET fluxes (i.e.,  $< 1.0$  mm d<sup>-1</sup>). This likely suggests the need to adjust the water availability factor ( $f_{WA}$ ) to positive values for a longer period, particularly at the end of the rainy season and beginning of the summer.

The annual ET, as estimated from both the RS-Met and EC, was higher than the total rainfall amount in some of the years studied (Fig. S3). A similar pattern was previously reported in forests in water-limited regions (Helman et al., 2017b; Raz-Yaseef et al., 2012; Williams et al., 2012). ET higher than rainwater supply indicates that trees use water stored in deep soil layers during wet years in the subsequent dry years (e.g., 2006 and 2008; Raz-Yaseef et al., 2012; Barbeta et al., 2015). Thus, the transfer of surplus rainwater from previous years should also be taken into consideration when adjusting the model with available water through the  $f_{WA}$  and  $f_{WD}$ , which are currently calculated only with the seasonal rainfall. Theoretically, this could be done by summing

the available water from the previous year (calculated as  $P - ET$ ) with the 2-month summed  $P$  in the calculation of the  $f_{WA}$  and  $f_{WD}$ . Of course, this would be applied only after completing the ET estimation of the first year.

The adjusted RS-Met GPP (i.e., that with the  $f_{WD}$ ) was also comparable to the GPP from the EC ( $765 \pm 112$  vs.  $748 \pm 124$  gC m<sup>-2</sup> yr<sup>-1</sup>, for GPP<sub>MOD</sub> and GPP<sub>EC</sub>, respectively) and highly correlated on an annual scale (Fig. 6a, b), with an  $R = 0.91$  ( $P < 0.001$ ;  $N = 9$ ) and a low mean absolute error (MAE) of  $52$  gC m<sup>-2</sup> yr<sup>-1</sup> (relative error of ca. 7%). MODIS GPP showed inferior correlation with EC estimates on an annual scale, with an  $R$  of 0.58 ( $P = 0.08$ ,  $N = 10$ ; Fig. 6c).

## 6 Testing the RS-Met across a rainfall gradient

### 6.1 Comparison with seasonal ET and GPP from EC and MODIS products

Next we compared the ET and GPP estimates from the RS-Met model with the field campaign data and MODIS ET and GPP products across the remaining six ecosystems. Comparison between estimates based on the RS-Met model, with and without the  $f_{WD}$ , with those from the EC indicated significantly higher correlations of the adjusted model (i.e., with the  $f_{WD}$ ) with EC estimates ( $P = 0.06$  and  $P < 0.01$  for ET and GPP, respectively; Table 2). Only the shrubland site of Kadita showed a higher ET correlation of EC with the unadjusted model. This was likely due to the continuous ET fluxes, which were not captured by the model, throughout the summer period at this relatively moist site.

In general, while using the  $f_{WD}$  did not improve (for the ET,  $P > 0.1$ , as indicated by a two-tailed Student's  $t$  test) or only marginally improved (for the GPP,  $P = 0.09$ , as indicated by a two-tailed Student's  $t$  test) RS-Met estimates at the non-forest sites, it significantly improved the ET and GPP estimates at forest sites ( $P = 0.05$  and  $P = 0.016$  for ET and GPP, respectively, as indicated by a two-tailed Student's  $t$  test). The adjusted RS-Met successfully tracked changes in ET and CO<sub>2</sub> fluxes from the dry to wet season at all sites. Similar to those shown in Yatir, MODIS ET and GPP fluxes were much lower than observed fluxes. This underestimation was particularly noted at the forest sites (Figs. 7 and S4).

Overall, the adjusted RS-Met was in good agreement with the EC measurements, with the cross-site regressions producing highly significant linear fits (Fig. 8a, b;  $R = 0.82$  and  $R = 0.86$ ; and MAE =  $0.47$  mm d<sup>-1</sup> and MAE =  $1.89$  gC m<sup>-2</sup> d<sup>-1</sup> for ET and GPP, respectively). Comparing between the EC vs. RS-Met regressions and the EC vs. MODIS ET and GPP regressions, using 8-day averaged fluxes values, produced the following linear fits:  $ET_{RS-Met} = 1.16 ET_{EC} - 0.11$  ( $R = 0.88$ ;  $P < 0.0001$ ;  $N = 36$ ),  $ET_{MODIS} = 0.38 ET_{EC} + 0.33$  ( $R = 0.65$ ;  $P < 0.0001$ ;  $N = 33$ ),  $GPP_{RS-Met} = 1.09 GPP_{EC} + 0.21$

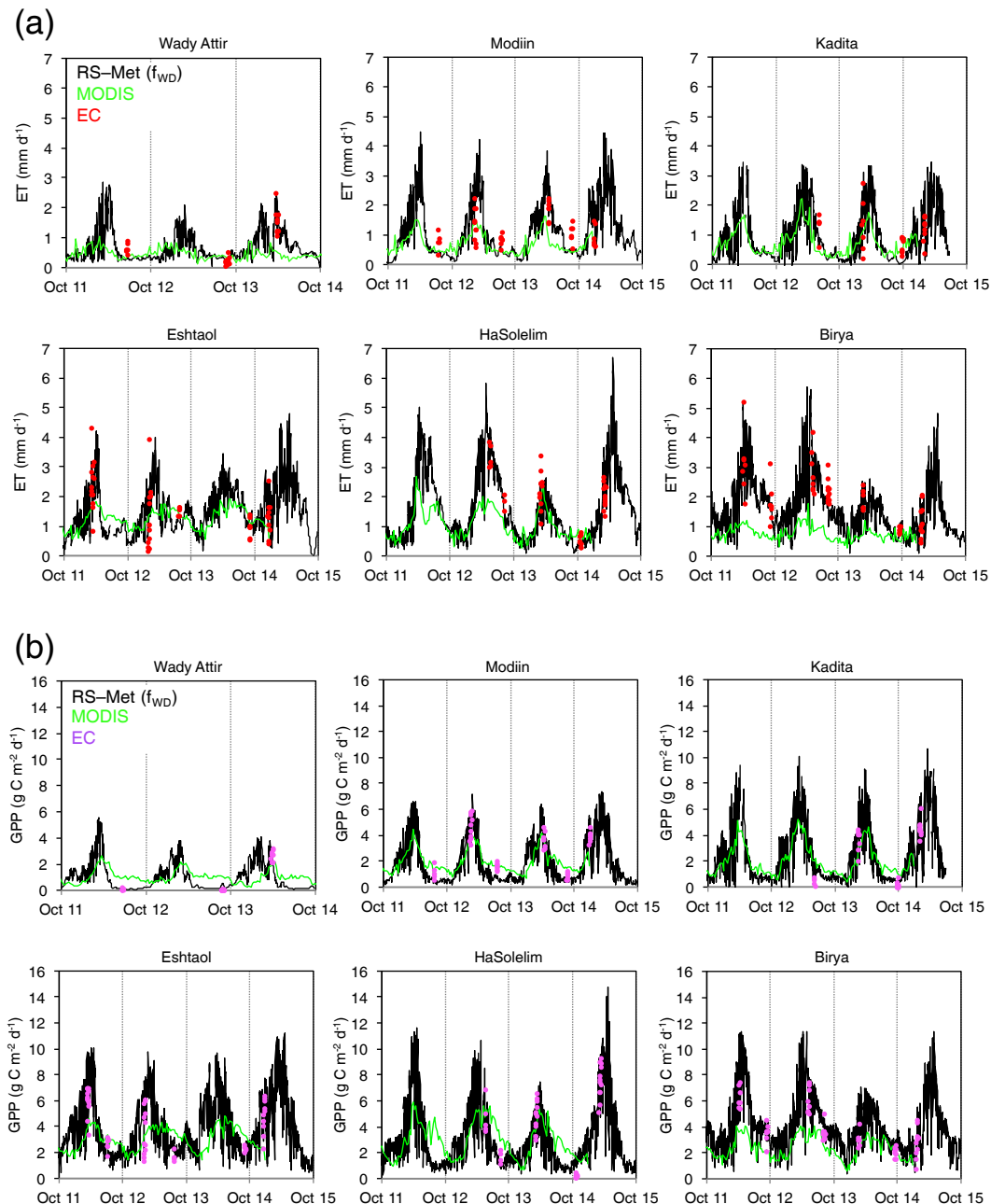


**Figure 7.** ET (a) and GPP (b) from EC, RS-Met (with  $f_{WD}$ ) and MODIS (MOD16A2 and MOD17A2 products) at the six forest and non-forested sites.

( $R = 0.92$ ;  $P < 0.0001$ ;  $N = 36$ ) and  $GPP_{MODIS} = 0.43 GPP_{EC} + 1.31$  ( $R = 0.77$ ;  $P < 0.0001$ ;  $N = 33$ ), showing a consistent underestimation of both MODIS products (MOD16 and MOD17) at those sites across sites (Fig. 8c, d).

The WUE (the slope of the regression between ET and GPP in Fig. S5) was slightly higher at  $2.32 \text{ g C kg}^{-1} \text{ H}_2\text{O}$  from the RS-Met compared to the low  $1.76 \text{ g C kg}^{-1} \text{ H}_2\text{O}$  from EC, but it was within the range reported for similar ecosystems in this region (Tang et al., 2014).

## 6.2 Annual-basis comparisons

To expand our analysis across the rainfall gradient, and because we do not have continuous estimations from the EC at the six sites, we compared the annual ET and GPP from the adjusted RS-Met with those from MODIS ET/GPP products. In the case of ET, we also added annual estimates derived from the empirical PaVI-E model (Helman et al., 2015).



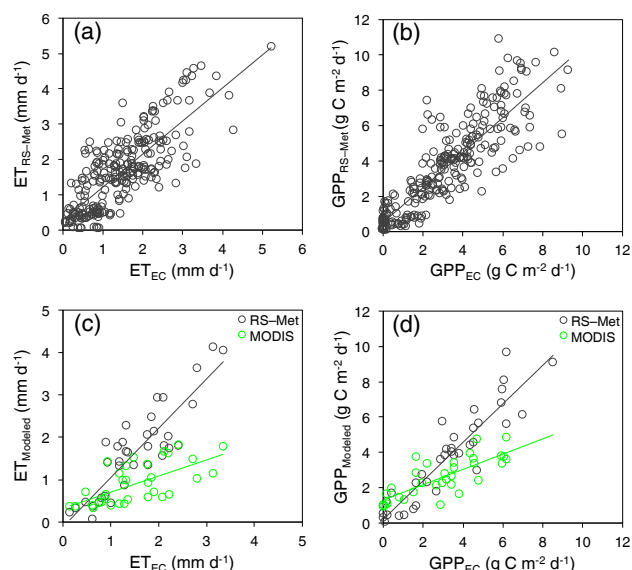


**Figure 8.** Cross-site EC vs. model correlations of ET (**a**, **c**) and GPP (**b**, **d**). In (**a**) and (**b**) are the EC vs. RS–Met (with  $f_{WD}$ ) values using all EC data from the six sites (each dot representing a single date), with linear fits of  $ET_{RS-Met} = 0.936 ET_{EC} + 0.281$  ( $R = 0.82$ ,  $P < 0.0001$ ,  $N = 243$ ) and  $GPP_{RS-Met} = 0.990 GPP_{EC} + 0.515$  ( $R = 0.86$ ,  $P < 0.0001$ ,  $N = 252$ ) for ET and GPP, respectively. In (**c**) and (**d**) are the same cross-site correlations but with data averaged over 8-day periods for comparisons with MODIS ET and GPP products (8-day averaged values). Linear fits for EC vs. RS–Met and MODIS in (**c**) are  $ET_{RS-Met} = 1.16 ET_{EC} - 0.11$  ( $R = 0.88$ ,  $P < 0.0001$ ,  $N = 36$ ) and  $ET_{MODIS} = 0.38 ET_{EC} + 0.33$  ( $R = 0.65$ ,  $P < 0.0001$ ,  $N = 33$ ), respectively. In (**d**), linear fits are  $GPP_{RS-Met} = 1.09 GPP_{EC} + 0.21$  ( $R = 0.92$ ,  $P < 0.0001$ ,  $N = 36$ ) and  $GPP_{MODIS} = 0.43 GPP_{EC} + 1.31$  ( $R = 0.77$ ,  $P < 0.0001$ ,  $N = 33$ ) for EC vs. RS–Met and MODIS, respectively.

The results of our ET comparison showed that the RS–Met and PaVI-E models produced comparable estimates at most of the sites (Fig. 9a), with the only exception being the drylands non-forest site of Wady Attir, which showed higher estimates from RS–Met than from PaVI-E ( $P < 0.01$ , as indicated by Tukey HSD separation procedure). MODIS ET was in accordance with estimates of RS–Met and PaVI-E at shrubland sites in spite of the underestimation of this product during the wet season likely due to the relatively higher ET at the beginning of the rainy season (Fig. 7a). However, MODIS ET was significantly lower than the other two models at the forest sites and also lower than the shrubland sites (Fig. 9a). The cross-site regression between the annual estimates from RS–Met vs. those from the EC produced a highly significant linear fit ( $R = 0.94$ ,  $P < 0.01$ ), confirming the potential use of the RS–Met in assessing ET on an annual scale across the rainfall gradient at those forest and non-forest sites.

MODIS GPP showed relatively comparable estimates to RS–Met on an annual scale due to its overestimation during

the dry season that compensated for its underestimation during the peak growth season (Fig. 9b). Here again, though, underestimation was observed at forest sites, particularly at the sites of Eshtaol and Biryia.

### 6.3 Changes in water use efficiency following afforestation across rainfall gradient

We finally used the adjusted RS–Met to assess the impact of afforestation on the water and carbon budgets across the rainfall gradient in Israel by comparing fluxes in three pine forests (i.e., Yatir, Eshtaol and Biryia) with those from the adjacent shrubland sites (i.e., Wady Attir, Modiin and Kadita, respectively). Results showed that the ET significantly increased due to the afforestation of these areas, particularly at the more humid site of Biryia (ca. 53 %), but to a lesser extent at the less humid site of Eshtaol (by ca. 20 %) and with almost no change in ET at the dryland site of Yatir (4 %). The GPP also significantly increased at those three paired sites. Overall, afforestation across the rainfall gradient was responsible for a significant increase in the WUE in this region (Fig. 10). Nevertheless, the positive change in the WUE decreased when moving from the dry Yatir–Wady Attir paired site ( $279 \text{ mm yr}^{-1}$ ) to the more humid paired site of Biryia–Kadita ( $766 \text{ mm yr}^{-1}$ ; Fig. 10), strengthening the importance of afforestation efforts in drylands areas.

## 7 Summary and conclusions

We have tested here a biophysical-based model of ET and CO<sub>2</sub> fluxes driven by satellite-derived vegetation index and meteorological data (RS–Met) and adjusted with a seasonal water deficit factor. The model was validated against direct flux measurements from extensive field campaigns and a fixed FLUXNET station and compared with MODIS ET and GPP products at seven evergreen forest and adjacent non-forested ecosystem sites along a steep rainfall gradient in the high-energy water-limited eastern Mediterranean region. Adjusting the model with the water deficit factor generally improved its performance compared to the model without the use of this factor, particularly at forest sites. The model also outperformed MODIS-based ET and GPP models, which showed generally lower estimates, particularly at the forest sites, suggesting that these models might benefit from the inclusion of the water deficit factor.

Our results show the potential use of this simple biophysical remote-sensing-based model in assessing ET and GPP on a daily basis and at a moderate spatial resolution of 250 m, even in high-energy water-limited Mediterranean environments. The addition of a water deficit factor (based on daily rainfall and radiation and/or temperature data alone) in the RS–Met significantly improved its performance in shrublands and especially in forests in this region and might be used in global vegetation models. Nevertheless, careful at-

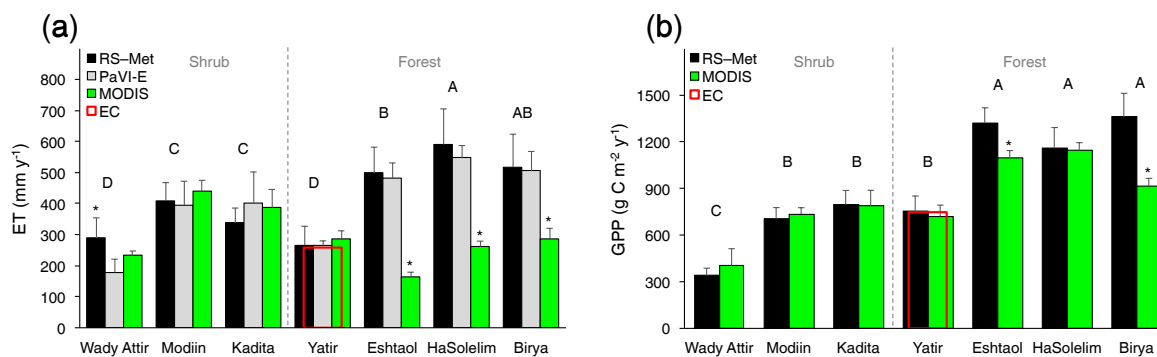


**Figure 9.** Mean annual (2003–2013) estimates of ET (a) and GPP (b) from RS–Met (black), MODIS (green) and PaVI–E (grey; only for ET in a; Helman et al., 2015a) at the seven sites. Uppercase letters indicate significant differences at  $P < 0.05$  between sites from the Tukey HSD separation procedure following two-way ANOVA for the interaction of site  $\times$  model (using PaVI–E and RS–Met in a and MODIS and RS–Met in b). Asterisks indicate significantly different values from other models for the specific site, as indicated by Tukey HSD. The EC annual sums at Yatir are also shown (red).

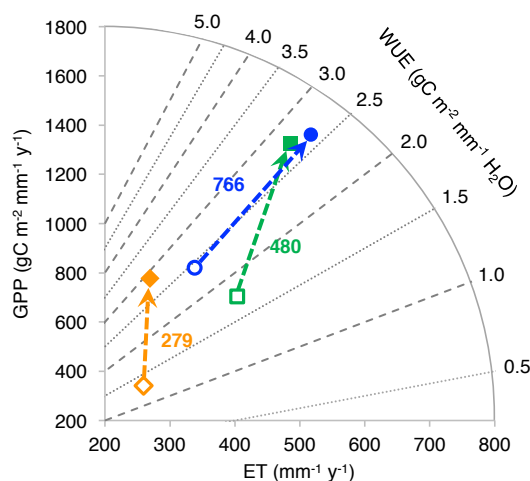


**Figure 10.** The change in GPP, ET and water use efficiency (WUE; as indicated by the direction of the arrow) attributed to the afforestation (closed symbols) of shrubland areas (open symbols) across a rainfall gradient in Israel (279–766 mm yr<sup>−1</sup>). The three paired forest and non-forest sites of Yatir–Wady Attir, Eshtaol–Modiin and Biryā–Kadita are indicated with yellow, green and blue colors, respectively. The rainfall level at each paired site is indicated near the arrow (mm yr<sup>−1</sup>). Note the changing slope of the change in ET and GPP, indicating that the gain in WUE due to afforestation decreases from dry to humid areas.

tention should be paid to adjusting the deficit water factor to local conditions, with its further development particularly required at the end of the rainy season and beginning of the dry period.

We lacked information on VPD at our sites, and thus excluded its simulated effects from the RS–Met model. However, there is much evidence that stomatal conductance is sensitive to VPD, with its effects usually accounted for in global vegetation models. Although temperature is tightly

interrelated with VPD, it is commonly suggested that VPD should also be considered in addition to temperature and soil moisture deficit in predicting plant-related biophysical processes such as transpiration and photosynthesis. By including the water deficit factor, we aimed here to indirectly account for these effects of VPD. However, RS–Met still showed a slight overestimation in the fluxes during the peak of the growth season (see results from Yatir site), when VPD is expected to be high. Thus, accounting for VPD effects on stomatal conductance in the RS–Met would have likely reduced these high fluxes during the period of high VPD conditions through the simulation of stomatal closure.

Further work should focus on refining the water deficit factor concept, including the contribution of VPD in the RS–Met. In addition, the contribution of direct surface evaporation from leaves should be accounted for with some sort of a factor adjusted to the seasonal development of the canopy leaf area (likely through the seasonal evolution of satellite-derived  $fVC$  and  $fAPAR$ ). The addition of a soil infiltration factor, adjusted with seasonal  $fVC$  and daily rainfall amount, should also probably be considered in the RS–Met. Eventually, a major challenge would be to apply the RS–Met globally, providing a global coverage of daily estimations of ET and CO<sub>2</sub> fluxes at a moderate spatial resolution.

Finally, using the RS–Met, we were able to estimate changes in water use efficiency due to afforestation across the rainfall gradient in Israel. Overall, afforestation across our study area was responsible for a significant increase in the WUE. However, the positive change in the WUE decreased when moving from dry (279 mm yr<sup>−1</sup>) to more humid (766 mm yr<sup>−1</sup>) regions, strengthening the importance of drylands afforestation.

The use of this simple approach linked to flexible campaign-based ground validation, as demonstrated in this study, represents a powerful basis for the reliable extension

of ET and GPP estimates across spatial and temporal scales in regions with a low density of flux stations.

*Data availability.* Data available upon request from corresponding author.

**The Supplement related to this article is available online at <https://doi.org/10.5194/bg-14-3909-2017-supplement>.**

*Competing interests.* The authors declare that they have no conflict of interest.

*Acknowledgements.* We thank the two anonymous referees for thoughtful comments and suggestions that contributed to the improvement of this paper. David Helman acknowledges personal grants provided by the Bar-Ilan University Presidential Office (Milgat Hanasi), the JNF–Rieger Foundation, USA, and the Hydrological Service of Israel, Water Authority. Shani Rohatyn acknowledges scholarships provided by the Ronnie Appleby fund, the Advanced School of Environmental Science of the Hebrew University and the Israel Ministry of Agriculture. We thank Efrat Ramati for helping with field work and data processing, Gerardo Fratini for helping with EddyPro, and Hagai Sagi and Avraham Perner for technical assistance. We are also grateful to the Meteorological Service of Israel for providing meteorological data and to NASA for making the MODIS NDVI datasets public. This research was partly supported by the Hydrological Service of Israel, Water Authority (grant no. 4500962964). Flux measurements were made possible through financial support from the Israel Science Foundation (ISF), Minerva foundation, JNF–KKL, the Hydrological Service of Israel, Water Authority, and the C. Wills and R. Lewis program in environmental science.

Edited by: Trevor Keenan

Reviewed by: two anonymous referees

## References

- Afik, T.: Quantitative estimation of CO<sub>2</sub> fluxes in a semi-arid forest and their dependence on climatic factors, Thesis submitted to R.H. Smith Faculty of Agriculture, Food and Environment of Hebrew University, Rehovot, Israel (in Hebrew), Thesis submitted to R.H. Smith Faculty of Agriculture, Food and Environment of Hebrew University, Rehovot, Israel, 2009 (in Hebrew).
- Ahlström, A., Raupach, M. R., Schurgers, G., Smith, B., Arneth, A., Jung, M., Reichstein, M., Canadell, J. G., Friedlingstein, P., Jain, A. K., Kato, E., Poulter, B., Sitch, S., Stocker, B. D., Viovy, N., Wang, Y. P., Wiltshire, A., Zaehle, S., and Zeng, N.: The dominant role of semi-arid ecosystems in the trend and variability of the land CO<sub>2</sub> sink, *Science*, 80, 348, 895–899, <https://doi.org/10.1126/science.aaa1668>, 2015.
- Allen, R. G., Pereira, L. S., and Raes, D.: Crop evapotranspiration?: guidelines for computing crop water requirements, FAO irrigation and drainage papers, 56, FAO, Rome, 1998.
- Allen, R. G., Pruitt, W. O., Wright, J. L., Howell, T. A., Ventura, F., Snyder, R., Itenfisu, D., Steduto, P., Berengena, J., Yrisarry, J. B., Smith, M., Pereira, L. S., Raes, D., Perrier, A., Alves, I., Walter, I., and Elliott, R.: A recommendation on standardized surface resistance for hourly calculation of reference ETo by the FAO56 Penman-Monteith method, *Agr. Water Manage.*, 81, 1–22, <https://doi.org/10.1016/j.agwat.2005.03.007>, 2006.
- Asaf, D., Rotenberg, E., Tatarinov, F., Dicken, U., Montzka, S. A., and Yakir, D.: Ecosystem photosynthesis inferred from measurements of carbonyl sulphide flux, *Nat. Geosci.*, 6, 186–190, 2013.
- Aubinet, M., Grelle, A., Ibrom, A., Rannik, S., Moncrieff, J., Foken, T., Kowalski, A. S., Martin, P. H., Berbigier, P., Bernhofer, C., Clement, R., Elbers, J. A., Granier, A., Grünwald, T., Morgenstern, K., Pilegaard, K., Rebmann, C., Snijders, W., Valentini, R., and Vesa, T.: Estimates of the annual net carbon and water exchange of forests: the EUROFLUX methodology, *Adv. Ecol. Res.*, 30, 113–175, 2000.
- Baldocchi, D. D.: Assessing the eddy covariance technique for evaluating carbon dioxide exchange rates of ecosystems: past, present and future, *Glob. Change Biol.*, 9, 479–492, 2003.
- Barbeta, A., Mejía-Chang, M., Ogaya, R., Voltas, J., Dawson, T. E., and Peñuelas, J.: The combined effects of a long-term experimental drought and an extreme drought on the use of plant-water sources in a Mediterranean forest, *Glob. Change Biol.*, 21, 1213–1225, <https://doi.org/10.1111/gcb.12785>, 2015.
- Ciais, P., Reichstein, M., Viovy, N., Granier, A., Ogée, J., Allard, V., Aubinet, M., Buchmann, N., Bernhofer, C., Carrara, a, Chevallier, F., De Noblet, N., Friend, A. D., Friedlingstein, P., Grünwald, T., Heinesch, B., Keronen, P., Knohl, a, Krinner, G., Loustau, D., Manca, G., Matteucci, G., Miglietta, F., Ourcival, J. M., Papale, D., Pilegaard, K., Rambal, S., Seufert, G., Soussana, J. F., Sanz, M. J., Schulze, E. D., Vesala, T., and Valentini, R.: Europe-wide reduction in primary productivity caused by the heat and drought in 2003, *Nature* 437, 529–533, <https://doi.org/10.1038/nature03972>, 2005.
- Cleveland, W. S.: Robust locally weighted regression and smoothing scatterplots, *J. Am. Stat. Assoc.*, 74, 829–836, 1979.
- Gamon, J. A., Field, C. B., Goulden, M. L., Griffin, K. L., Hartley, A. E., Joel, G., Peñuelas, J., and Valentini, R.: Relationships between NDVI, canopy structure, and photosynthesis in three Californian vegetation types, *Ecol. Appl.*, 28–41, 1995.
- Garbulsky, M. F., Penuelas, J., Papale, D., and Filella, I.: Remote estimation of carbon dioxide uptake by a Mediterranean forest, *Glob. Change Biol.*, 14, 2860–2867, <https://doi.org/10.1111/j.1365-2486.2008.01684.x>, 2008.
- Garbulsky, M. F., Filella, I., Verger, A., and Peñuelas, J.: Photosynthetic light use efficiency from satellite sensors: From global to Mediterranean vegetation, *Environ. Exp. Bot.*, 103, 3–11, <https://doi.org/10.1016/j.envexpbot.2013.10.009>, 2014.
- Glenn, E., Nagler, P., and Huete, A.: Vegetation Index Methods for Estimating Evapotranspiration by Remote Sensing, *Surv. Geophys.*, 31, 531–555, <https://doi.org/10.1007/s10712-010-9102-2>, 2010.
- Glenn, E. P., Huete, A. R., Nagler, P. L., and Nelson, S. G.: Relationship Between Remotely-sensed Vegetation Indices, Canopy Attributes and Plant Physiological Processes: What Vegetation

- Indices Can and Cannot Tell Us About the Landscape, *Sensors*, 8, 2136–2160, <https://doi.org/10.3390/s8042136>, 2008.
- Glenn, E. P., Neale, C. M. U., Hunsaker, D. J., and Naylor, P. L.: Vegetation index-based crop coefficients to estimate evapotranspiration by remote sensing in agricultural and natural ecosystems, *Hydrol. Process.*, 25, 4050–4062, <https://doi.org/10.1002/hyp.8392>, 2011.
- Helman, D.: Land Surface Phenology: What do we really “see” from space?, *Total Environ.*, accepted, <https://doi.org/10.1016/j.scitotenv.2017.07.237>, 2017.
- Helman, D., Lensky, I. M., Mussery, A., and Leu, S.: Rehabilitating degraded drylands by creating woodland islets: Assessing long-term effects on aboveground productivity and soil fertility, *Agr. Forest Meteorol.*, 195–196, 52–60, <https://doi.org/10.1016/j.agrformet.2014.05.003>, 2014a.
- Helman, D., Mussery, A., Lensky, I. M., and Leu, S.: Detecting changes in biomass productivity in a different land management regimes in drylands using satellite-derived vegetation index, *Soil Use Manag.*, 30, 32–39, <https://doi.org/10.1111/sum.12099>, 2014b.
- Helman, D., Givati, A., and Lensky, I. M.: Annual evapotranspiration retrieved from satellite vegetation indices for the eastern Mediterranean at 250 m spatial resolution, *Atmos. Chem. Phys.*, 15, 12567–12579, <https://doi.org/10.5194/acp-15-12567-2015>, 2015a.
- Helman, D., Lensky, I. M., Tessler, N., and Osem, Y.: A phenology-based method for monitoring woody and herbaceous vegetation in Mediterranean forests from NDVI time series, *Remote Sens.*, 7, 12314–12335, <https://doi.org/10.3390/rs70912314>, 2015b.
- Helman, D., Osem, Y., Yakir, D., and Lensky, I. M.: Relationships between climate, topography, water use and productivity in two key Mediterranean forest types with different water-use strategies, *Agr. Forest Meteorol.*, 232, 319–330, <https://doi.org/10.1016/j.agrformet.2016.08.018>, 2017a.
- Helman, D., Lensky, I. M., Yakir, D., and Osem, Y.: Forests growing under dry conditions have higher hydrological resilience to drought than do more humid forests, *Glob. Change Biol.*, 23, 2801–2817, <https://doi.org/10.1111/gcb.13551>, 2017b.
- Helman, D., Leu, S., and Mussery, A.: Contrasting effects of two *Acacia* species on understorey growth in a drylands environment: Interplay of canopy shading and litter interference, *J. Veg. Sci.*, <https://doi.org/10.1111/jvs.12576>, 2017c.
- Hilker, T., Coops, N. C., Wulder, M. A., Black, T. A., and Guy, R. D.: The use of remote sensing in light use efficiency based models of gross primary production: A review of current status and future requirements, *Sci. Total Environ.*, 404, 411–423, <https://doi.org/10.1016/j.scitotenv.2007.11.007>, 2008.
- Huete, A., Didan, K., Miura, T., Rodriguez, E. P., Gao, X., and Ferreira, L. G.: Overview of the radiometric and biophysical performance of the MODIS vegetation indices, *Remote Sens. Environ.*, 83, 195–213, 2002.
- Jensen, M. E. and Haise, H. R.: Estimating evapotranspiration from solar radiation, *Proc. Am. Soc. Civ. Eng. J. Irrig. Drain. Div.*, 89, 15–41, 1963.
- Jung, M., Reichstein, M., Ciais, P., Seneviratne, S. I., Sheffield, J., Goulden, M. L., Bonan, G., Cescatti, A., Chen, J., de Jeu, R., Dolman, A. J., Eugster, W., Gerten, D., Gianelle, D., Gobron, N., Heinke, J., Kimball, J., Law, B. E., Montagnani, L., Mu, Q., Mueller, B., Oleson, K., Papale, D., Richardson, A. D., Rouspard, O., Running, S., Tomelleri, E., Viovy, N., Weber, U., Williams, C., Wood, E., Zaehle, S., and Zhang, K.: Recent decline in the global land evapotranspiration trend due to limited moisture supply, *Nature*, 467, 951–954, <https://doi.org/10.1038/nature09396>, 2010.
- Kalma, J., McVicar, T., and McCabe, M.: Estimating Land Surface Evaporation: A Review of Methods Using Remotely Sensed Surface Temperature Data, *Surv. Geophys.*, 29, 421–469, <https://doi.org/10.1007/s10712-008-9037-z>, 2008.
- Klein, T., Rotenberg, E., Tatarinov, F., and Yakir, D.: Association between sap flow-derived and eddy covariance-derived measurements of forest canopy CO<sub>2</sub> uptake, *New Phytol.*, 209, 436–446, <https://doi.org/10.1111/nph.13597>, 2016.
- Kool, D., Agam, N., Lazarovitch, N., Heitman, J. L., Sauer, T. J., and Ben-Gal, A.: A review of approaches for evapotranspiration partitioning, *Agr. Forest Meteorol.*, 184, 56–70, <https://doi.org/10.1016/j.agrformet.2013.09.003>, 2014.
- Leu, S., Mussery, A., and Budovsky, A.: The effects of long time conservation of heavily grazed shrubland: A case study in the Northern Negev, Israel, *Environ. Manage.*, 54, 309–319, 2014.
- Llusia, J., Rohtyn, S., Yakir, D., Rotenberg, E., Seco, R., Guenther, A., and Peñuelas, J.: Photosynthesis, stomatal conductance and terpene emission response to water availability in dry and mesic Mediterranean forests, *Trees*, 30, 749–759, <https://doi.org/10.1007/s00468-015-1317-x>, 2016.
- Maselli, F., Barbati, A., Chiesi, M., Chirici, G., and Corona, P.: Use of remotely sensed and ancillary data for estimating forest gross primary productivity in Italy, *Remote Sens. Environ.*, 100, 563–575, <https://doi.org/10.1016/j.rse.2005.11.010>, 2006.
- Maselli, F., Papale, D., Puletti, N., Chirici, G., and Corona, P.: Combining remote sensing and ancillary data to monitor the gross productivity of water-limited forest ecosystems, *Remote Sens. Environ.*, 113, 657–667, <https://doi.org/10.1016/j.rse.2008.11.008>, 2009.
- Maselli, F., Papale, D., Chiesi, M., Matteucci, G., Angeli, L., Raschi, A., and Seufert, G.: Operational monitoring of daily evapotranspiration by the combination of MODIS NDVI and ground meteorological data: Application and evaluation in Central Italy, *Remote Sens. Environ.*, 152, 279–290, <https://doi.org/10.1016/j.rse.2014.06.021>, 2014.
- Maseyk, K., Hemming, D., Angert, A., Leavitt, S. W., and Yakir, D.: Increase in water-use efficiency and underlying processes in pine forests across a precipitation gradient in the dry Mediterranean region over the past 30 years, *Oecologia*, 167, 573–585, <https://doi.org/10.1007/s00442-011-2010-4>, 2011.
- Maseyk, K. S., Lin, T., Rotenberg, E., Grünzweig, J. M., Schwartz, A., and Yakir, D.: Physiology-phenology interactions in a productive semi-arid pine forest, *New Phytol.*, 178, 603–616, 2008.
- Monteith, J. L.: Climate and the efficiency of crop production in Britain, *Philos. T. R. Soc. Lond. B*, 281, 277–294, 1977.
- Mu, Q., Heinsch, F. A., Zhao, M., and Running, S. W.: Development of a global evapotranspiration algorithm based on MODIS and global meteorology data, *Remote Sens. Environ.*, 111, 519–536, <https://doi.org/10.1016/j.rse.2006.07.007>, 2007.
- Mu, Q., Zhao, M., and Running, S. W.: Improvements to a MODIS global terrestrial evapotranspiration algorithm, *Remote Sens. Environ.*, 115, 1781–1800, <https://doi.org/10.1016/j.rse.2011.02.019>, 2011.

- Mussery, A., Helman, D., Leu, S., and Budovsky, A.: Modeling herbaceous productivity considering tree-grass interactions in drylands savannah: The case study of Yatir farm in the Negev drylands, *J. Arid Environ.*, 124, 160–164, <https://doi.org/10.1016/j.jaridenv.2015.08.013>, 2016.
- Myneni, R. B. and Williams, D. L.: On the relationship between FAPAR and NDVI, *Remote Sens. Environ.*, 49, 200–211, [https://doi.org/10.1016/0034-4257\(94\)90016-7](https://doi.org/10.1016/0034-4257(94)90016-7), 1994.
- Nagaraja Rao, C. R.: Photosynthetically active components of global solar radiation: Measurements and model computations, *Arch. Meteorol. Geophys. B*, 34, 353–364, <https://doi.org/10.1007/BF02269448>, 1984.
- Osem, Y., Zangy, E., Bney-Moshe, E., and Moshe, Y.: Understory woody vegetation in manmade Mediterranean pine forests: variation in community structure along a rainfall gradient, *Eur. J. Forest Res.*, 131, 693–704, <https://doi.org/10.1007/s10342-011-0542-0>, 2012.
- Peñuelas, J., Garbulsky, M. F., and Filella, I.: Photochemical reflectance index (PRI) and remote sensing of plant CO<sub>2</sub> uptake, *New Phytol.*, 191, 596–599, <https://doi.org/10.1111/j.1469-8137.2011.03791.x>, 2011.
- Raz-Yaseef, N., Yakir, D., Schiller, G., and Cohen, S.: Dynamics of evapotranspiration partitioning in a semi-arid forest as affected by temporal rainfall patterns, *Agr. Forest Meteorol.*, 157, 77–85, <https://doi.org/10.1016/j.agrformet.2012.01.015>, 2012.
- Reichstein, M., Falge, E., Baldocchi, D., Papale, D., Aubinet, M., Berbigier, P., Bernhofer, C., Buchmann, N., Gilmanov, T., Granier, A., Grünwald, T., Havránek, K., Ilvesniemi, H., Janous, D., Knohl, A., Laurila, T., Lohila, A., Loustau, D., Matteucci, G., Meyers, T., Miglietta, F., Ourcival, J.-M., Pumpanen, J., Rambal, S., Rotenberg, E., Sanz, M., Tenhunen, J., Seufert, G., Vaccari, F., Vesala, T., Yakir, D., and Valentini, R.: On the separation of net ecosystem exchange into assimilation and ecosystem respiration: review and improved algorithm, *Glob. Change Biol.*, 11, 1424–1439, <https://doi.org/10.1111/j.1365-2486.2005.001002.x>, 2005.
- Reichstein, M., Bahn, M., Ciais, P., Frank, D., Mahecha, M. D., Seneviratne, S. I., Zscheischler, J., Beer, C., Buchmann, N., Frank, D. C., Papale, D., Rammig, A., Smith, P., Thonicke, K., Velde, M. van der, Vicca, S., Walz, A., and Wattenbach, M.: Climate extremes and the carbon cycle, *Nature*, 500, 287–295, <https://doi.org/10.1038/nature12350>, 2013.
- Rotenberg, E. and Yakir, D.: Distinct patterns of changes in surface energy budget associated with forestation in the semiarid region, *Glob. Change Biol.*, 17, 1536–1548, <https://doi.org/10.1111/j.1365-2486.2010.02320.x>, 2011.
- Running, S. W. and Nemani, R. R.: Relating seasonal patterns of the AVHRR vegetation index to simulated photosynthesis and transpiration of forests in different climates, *Remote Sens. Environ.*, 24, 347–367, [https://doi.org/10.1016/0034-4257\(88\)90034-X](https://doi.org/10.1016/0034-4257(88)90034-X), 1988.
- Running, S. W., Thornton, P. E., Nemani, R., and Glassy, J. M.: Global Terrestrial Gross and Net Primary Productivity from the Earth Observing System, in: *Methods in Ecosystem Science*, edited by: Sala, O. E., Jackson, R. B., Mooney, H. A., and Howarth, R. W., 44–57, 2000.
- Running, S. W., Nemani, R. R., Heinsch, F. A., Zhao, M., Reeves, M., and Hashimoto, H.: A Continuous Satellite-Derived Measure of Global Terrestrial Primary Production, *Bioscience*, 54, 547–560, [https://doi.org/10.1641/0006-3568\(2004\)054\[0547:ACSMOG\]2.0.CO;2](https://doi.org/10.1641/0006-3568(2004)054[0547:ACSMOG]2.0.CO;2), 2004.
- Schimel, D., Pavlick, R., Fisher, J. B., Asner, G. P., Saatchi, S., Townsend, P., Miller, C., Frankenberg, C., Hibbard, K., and Cox, P.: Observing terrestrial ecosystems and the carbon cycle from space, *Glob. Change Biol.*, 21, 1762–1776, <https://doi.org/10.1111/gcb.12822>, 2015.
- Sims, D. A., Rahman, A. F., Cordova, V. D., El-Masri, B. Z., Baldocchi, D. D., Bolstad, P. V., Flanagan, L. B., Goldstein, A. H., Hollinger, D. Y., Misson, L., Monson, R. K., Oechel, W. C., Schmid, H. P., Wofsy, S. C., and Xu, L.: A new model of gross primary productivity for North American ecosystems based solely on the enhanced vegetation index and land surface temperature from MODIS, *Remote Sens. Data Assim. Spec. Issue*, 112, 1633–1646, <https://doi.org/10.1016/j.rse.2007.08.004>, 2008.
- Spritsin, M., Cohen, S., Maseyk, K., Rotenberg, E., Grünzweig, J., Karnieli, A., Berliner, P., and Yakir, D.: Long term and seasonal courses of leaf area index in a semi-arid forest plantation, *Agr. Forest Meteorol.*, 151, 565–574, <https://doi.org/10.1016/j.agrformet.2011.01.001>, 2011.
- Tang, X., Li, H., Desai, A. R., Nagy, Z., Luo, J., Kolb, T. E., Olioso, A., Xu, X., Yao, L., Kutsch, W., Pilegaard, K., Köstner, B., and Ammann, C.: How is water-use efficiency of terrestrial ecosystems distributed and changing on Earth?, *Sci. Rep.*, 4, 7483, <https://doi.org/10.1038/srep07483>, 2014.
- Tatarinov, F., Rotenberg, E., Maseyk, K., Ogée, J., Klein, T., and Yakir, D.: Resilience to seasonal heat wave episodes in a Mediterranean pine forest, *New Phytol.*, 210, 485–496, <https://doi.org/10.1111/nph.13791>, 2016.
- Veroustraete, F., Sabbe, H., and Eerens, H.: Estimation of carbon mass fluxes over Europe using the C-Fix model and Euroflux data, *Remote Sens. Environ.*, 83, 376–399, <https://doi.org/10.1016/j.ecolmodel.2006.06.008>, 2002.
- Wang, H., Zhao, P., Zou, L. L., McCarthy, H. R., Zeng, X. P., Ni, G. Y., and Rao, X. Q.: CO<sub>2</sub> uptake of a mature *Acacia mangium* plantation estimated from sap flow measurements and stable carbon isotope discrimination, *Biogeosciences*, 11, 1393–1411, <https://doi.org/10.5194/bg-11-1393-2014>, 2014.
- Way, D. A., Oren, R., and Kroner, Y.: The space-time continuum: the effects of elevated CO<sub>2</sub> and temperature on trees and the importance of scaling, *Plant. Cell Environ.*, 38, 991–1007, <https://doi.org/10.1111/pce.12527>, 2015.
- Williams, C. A., Reichstein, M., Buchmann, N., Baldocchi, D., Beer, C., Schwalm, C., Wohlfahrt, G., Hasler, N., Bernhofer, C., Foken, T., Papale, D., Schymanski, S., and Schaefer, K.: Climate and vegetation controls on the surface water balance: Synthesis of evapotranspiration measured across a global network of flux towers, *Water Resour. Res.*, 48, W06523, <https://doi.org/10.1029/2011WR011586>, 2012.
- Wu, C., Huang, W., Yang, Q., and Xie, Q.: Improved estimation of light use efficiency by removal of canopy structural effect from the photochemical reflectance index (PRI), *Agr. Ecosyst. Environ.*, 199, 333–338, <https://doi.org/10.1016/j.agee.2014.10.017>, 2015.
- Zhao, M. and Running, S. W.: Drought-Induced Reduction in Global Terrestrial Net Primary Production from 2000 Through 2009, *Science*, 329, 940–943, 2010.